


Article

Duodenal Metabolic Profile Changes in Heat-Stressed Broilers

Jalila S. Dridi¹, Elizabeth S. Greene², Craig W. Maynard², Giorgio Brugaletta^{2,3}, Alison Ramser², Courtney J. Christopher⁴, Shawn R. Campagna^{4,5}, Hector F. Castro⁵ and Sami Dridi^{2,*} 

- ¹ École Universitaire de Kinésithérapie, Université d'Orléans, Rue de Chartres, 45100 Orléans, France; jaliladr2@gmail.com
- ² Center of Excellence for Poultry Science, University of Arkansas, Fayetteville, AR 72701, USA; esgreene@uark.edu (E.S.G.); cwmaynar@uark.edu (C.W.M.); giorgiob@uark.edu (G.B.); atramser@uark.edu (A.R.)
- ³ Department of Agricultural and Food Sciences, Alma Mater Studiorum, University of Bologna, 40064 Bologna, Italy
- ⁴ Department of Chemistry, University of Tennessee, Knoxville, TN 37996, USA; cleathe3@vols.utk.edu (C.J.C.); campagna@utk.edu (S.R.C.)
- ⁵ Biological and Small Molecule Mass Spectrometry Core, University of Tennessee, Knoxville, TN 37996, USA; hcastrog@utk.edu
- * Correspondence: dridi@uark.edu; Tel.: +(479)-575-2583; Fax: +(479)-575-7139

Simple Summary: Heat stress (HS) represents an environmental and socio-economic burden to the poultry industry worldwide. However, the underpinning mechanisms for HS responses are still not well defined. Here, we used a high-throughput analysis to determine the metabolite profiles in acute and chronic heat-stressed broilers in comparison with thermoneutral and pair-fed birds. The results showed that HS altered several duodenal metabolites in a duration-dependent manner and identified potential metabolite signatures.



Citation: Dridi, J.S.; Greene, E.S.; Maynard, C.W.; Brugaletta, G.; Ramser, A.; Christopher, C.J.; Campagna, S.R.; Castro, H.F.; Dridi, S. Duodenal Metabolic Profile Changes in Heat-Stressed Broilers. *Animals* **2022**, *12*, 1337. <https://doi.org/10.3390/ani12111337>

Academic Editors: João Carlos Caetano Simões and Ana Cristina Silvestre Ferreira

Received: 28 March 2022

Accepted: 19 May 2022

Published: 24 May 2022

Publisher's Note: MDPI stays neutral with regard to jurisdictional claims in published maps and institutional affiliations.



Copyright: © 2022 by the authors. Licensee MDPI, Basel, Switzerland. This article is an open access article distributed under the terms and conditions of the Creative Commons Attribution (CC BY) license (<https://creativecommons.org/licenses/by/4.0/>).

Abstract: Heat stress (HS) is devastating to poultry production sustainability worldwide. In addition to its adverse effects on growth, welfare, meat quality, and mortality, HS alters the gut integrity, leading to dysbiosis and leaky gut syndrome; however, the underlying mechanisms are not fully defined. Here, we used a high-throughput mass spectrometric metabolomics approach to probe the metabolite profile in the duodenum of modern broilers exposed to acute (AHS, 2 h) or chronic cyclic (CHS, 8 h/day for 2 weeks) HS in comparison with thermoneutral (TN) and pair-fed birds. Ultra high performance liquid chromatography coupled with high resolution mass spectrometry (UHPLC–HRMS) identified a total of 178 known metabolites. The trajectory analysis of the principal component analysis (PCA) score plots (both 2D and 3D maps) showed clear separation between TN and each treated group, indicating a unique duodenal metabolite profile in HS birds. Within the HS groups, partial least squares discriminant analysis (PLS-DA) displayed different clusters when comparing metabolite profiles from AHS and CHS birds, suggesting that the metabolite signatures were also dependent on HS duration. To gain biologically related molecule networks, the above identified duodenal metabolites were mapped into the Ingenuity Pathway Analysis (IPA) knowledge-base and analyzed to outline the most enriched biological functions. Several common and specific top canonical pathways were generated. Specifically, the adenosine nucleotide degradation and dopamine degradation pathways were specific for the AHS group; however, the UDP-D-xylose and UDP-D-glucuronate biosynthesis pathways were generated only for the CHS group. The top diseases enriched by the IPA core analysis for the DA metabolites, including cancer, organismal (GI) injury, hematological, cardiovascular, developmental, hereditary, and neurological disorders, were group-specific. The top altered molecular and cellular functions were amino acid metabolism, molecular transport, small molecule biochemistry, protein synthesis, cell death and survival, and DNA damage and repair. The IPA-causal network predicted that the upstream regulators (carnitine palmitoyltransferase 1B, CPT1B; histone deacetylase 11, HDAC11; carbonic anhydrase 9, CA9; interleukin 37, IL37; glycine N-methyl transferase, GNMT; GATA4) and the downstream mediators (mitogen-activated protein kinases, MAPKs; superoxide dismutase, SOD) were altered in the HS groups. Taken together, these data showed that, independently of feed intake depression, HS induced

significant changes in the duodenal metabolite profile in a duration-dependent manner and identified a potential duodenal signature for HS.

Keywords: heat stress; broilers; metabolomics; canonical pathways; mass spectrometry

1. Introduction

Poultry meat is highly regarded as an efficient source for high quality proteins with affordable prices and without religious taboos. With a global annual average production of $99,901 \times 10^3$ metric tons [1], strengthened by intensive genetic selection and long-term genetic gain (growth rate, breast yield, feed efficiency) and improvement of housing and management, broiler (meat-type) chickens are a central component of the worldwide meat production market and support the livelihoods and food security of billions of people. However, these unprecedented and successful advances were associated with several unexpected and undesirable changes, such as the emergence of metabolic disorders (muscle myopathies, etc.) and hypersensitivity to high environmental temperatures [2,3].

Climate change and global warming are real concerns, as unusually warm hot seasons and temperature anomalies have markedly increased and broadened over the past decades [4–8]. Global warming and heat stress are adversely affecting every biological system, including birds, large animals, insects, and crops, and thereby threatening the sustainability of global agricultural production [8–11]. Of particular interest, broiler chickens are very susceptible to heat stress, as they lack sweat glands, are covered with feathers, and have high metabolic activity and core body temperatures [12–14]. The strong adverse effects of heat stress on poultry performance, well-being, mortality, meat yield and quality are well documented [15–21]. One of the prominent negative effects of heat stress is gut injury; however, its underlying mechanisms are not well understood [22,23]. The brain–gut axis, involving the enteric nervous system (ENS), the autonomic nervous system (ANS), the hypothalamus–pituitary axis (HPA), and the central nervous system (CNS), is very responsive to any stress, including heat load [24–27]. Although the complexity of the brain–gut interactions, functionality, and network is still at the beginning of unraveling, there is evidence that heat stress triggers the activation of HPA and ANS, leading to increased corticosterone levels and pro-inflammatory cytokines, which in turn affect the intestinal homeostatic functions [28]. For instance, it has been shown that the abovementioned changes, in combination with depressed feed intake induced by heat stress, alter gut motility, flux patterns, secretory activity, content viscosity, and pH [23,29,30].

It is important to highlight that, to dissipate heat during high ambient temperature, heat-stressed birds divert blood flow to the periphery (skin) [31–34]. This, in turn, leads to a hypoxia-like state in several internal organs, including the gut [35,36]. Combined with low nutrient supply, which is exacerbated by depression in energy intake, hypoxia would result in adenosine triphosphate (ATP) depletion, promoting oxidative and nitrosative stress that leads to leaky gut syndrome [37–39]. The integrity of the intestinal barrier and its effective functionality are vital for the overall health and performance of broilers [40–42]. As heat stress is a global socio-economic burden that jeopardizes poultry welfare, profitability, and global food security, and as larger and widespread heat waves are predicted for the next century [43–45], there is a critical need to define the mechanisms of heat stress responses and their effect on poultry intestinal permeability.

In previous studies, we have shown that heat stress alters the expression of intestinal heat-shock proteins, cyto(chemo)kines, tight junction proteins, and nutrient transporters, thereby inducing leaky gut syndrome [15,46,47]. To gain further in-depth insights into heat stress responses and intestinal barrier integrity, we undertook the present study using an ultra-high performance liquid chromatography–high resolution mass spectrometry (UHPLC–HRMS) based metabolomics approach to determine the metabolic profile in the

duodenum of modern broilers exposed to acute (2 h) or chronic cyclic (8 h/day for 2 weeks) heat stress in comparison with thermoneutral and pair-fed birds.

2. Materials and Methods

2.1. Ethics Statements

The present study was conducted in accordance with the recommendations in the guide for the care and use of laboratory animals of the National Institutes of Health, and the protocol was approved by the Institutional Animal Care and Use Committee (#21050) at the University of Arkansas.

2.2. Birds, Diets, and Heat Stress Challenge

One-day old male broiler (meat-type) chicks ($n = 672$) were obtained from commercial Cobb-Vantress hatchery (Siloam Springs, Arkansas), neck tagged, individually weighed, and randomly allocated to 12 environmental chambers (2 floor pens/chamber, 24 pens in total, 28 birds/pen). Each pen was covered with 7 cm fresh pine shavings and equipped with a plastic hanging poultry feeder and an automatic vacuum-sealing O-ring drinker. Birds were given *ad libitum* access to clean and fresh water and a corn–soybean meal basal diet (starter d 1–14, grower d 15–28, and finisher d 29–42). The diet composition has been previously described [15]. Temperature was maintained at 32 °C for the first 3 days, and then gradually reduced approximately 3 °C each week until it reached 23 °C on d 21. The average relative humidity was 30%. The lighting program was 24 h light for the first 3 days, reduced to 23 h light:1 h dark during d 4–7, and reduced further to 18 h light: 6 h dark thereafter. The experiment followed a completely randomized design with three treatments (8 replicate pens/treatment): a control group (TN) where the birds were raised under thermoneutral condition (23 °C) from d 29–42, a chronic cyclic heat-stressed group (CHS) where the birds were exposed to high ambient temperature (35 °C) for 8 h/d (9:30 am to 5:30 pm) from d 29–42 to mimic summer time in Arkansas, and a pair-fed group (PF) where the birds were raised like the control group (similar environmental conditions, 23 °C) and fed the same amount of feed as the CHS group. Using the pair-fed TN group would help to distinguish between the effect of feed depression and the effect of heat stress. Feed intake and water consumption were recorded daily. Individual body weight was recorded weekly. Body core temperature was continuously monitored using Thermochron temperature logger (iButton, DS19221, Embedded Data Systems, Lawrenceburg, KY, USA). The environmental temperature and humidity were also continuously recorded in each chamber. At the end of the experiment (d 42), duodenum segments from each group (TN, CHS, PF, $n = 8$ /group) were collected, rinsed in PBS 1x, snap frozen in liquid nitrogen, and stored at –80 °C for metabolomics analysis. Duodenum sections were also collected from two additional groups: an acute heat-stressed group (AHS), where some TN birds were exposed to 35 °C for 2 h before sampling on d 42, and a preheat-stressed group (PHS), where CHS birds were sampled before starting the heat stress on d 42 (Figure 1).

2.3. Sample Collection and Preparation

Duodenum tissues were ground, snap frozen in liquid nitrogen, and sent to the Biological and Small Molecule Mass Spectrometry Core (BSMMSC, The University of Tennessee, Knoxville, TN, USA). Metabolites were extracted with 1.5 mL of extraction solvent (40:40:20 HPLC grade methanol: acetonitrile: water with formic acid at a final concentration of 0.1 M), pre-chilled at 4 °C, and incubated at –20 °C for 20 min. Samples were centrifuged ($13,300\times g$, 5 min, 4 °C), and supernatants were collected. Solvent was evaporated under a stream of nitrogen, and metabolites were suspended with 300 μ L of HPLC-grade water prior to mass analysis.

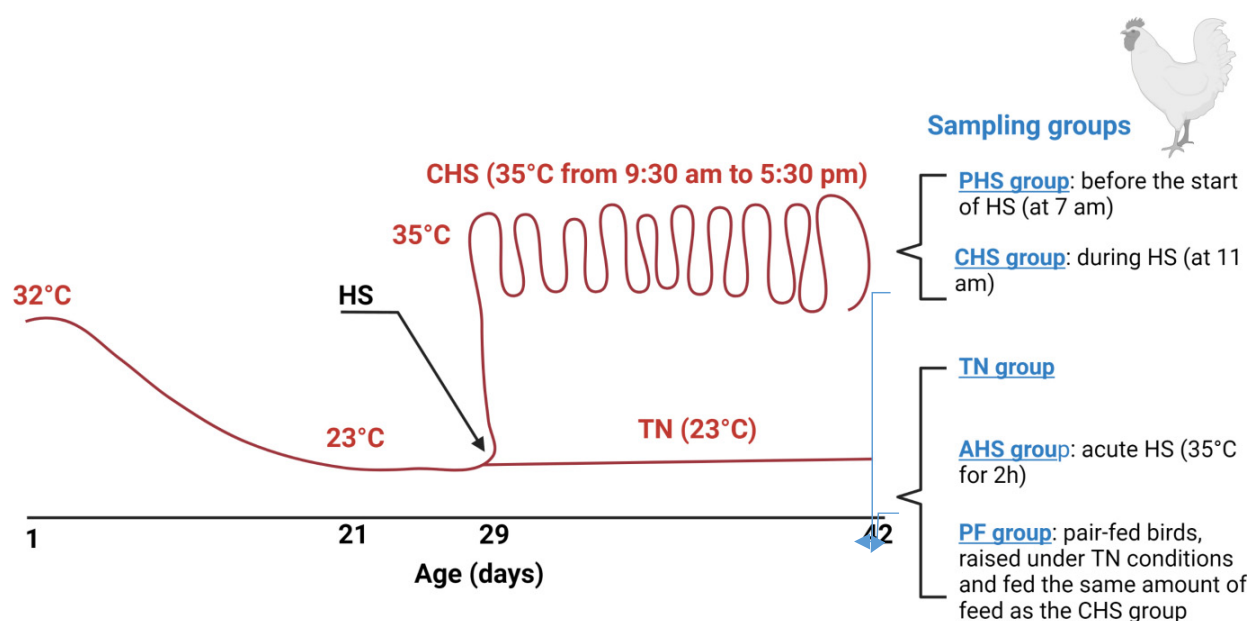


Figure 1. Experimental design representation and heat stress challenge. Temperature was gradually reduced from 32 °C to approximately 23 °C on d 21. At d 29, the experiment followed a completely randomized design with three treatments (8 replicate pens/treatment, 28 birds/pen): a control group (TN) where the birds were raised under thermoneutral condition (23 °C) from d 29–42, a chronic cyclic heat-stressed group (CHS) where the birds were exposed to high ambient temperature (35 °C) for 8 h/d (9:30 am to 5:30 pm) from d 29–42, and a pair-fed group (PF) where the birds were raised like the control group (similar environmental conditions, 23 °C) and fed the same amount of feed as the CHS group. Two additional groups were also used: an acute heat-stressed group (AHS) where some TN birds were exposed to 35 °C for 2 h before sampling on d 42, and a preheat-stressed group (PHS) where CHS birds were sampled before starting the heat stress on d 42. AHS, acute heat stress; CHS, chronic cyclic heat stress; HS, heat stress; PHS, preheat stress; PF, pair fed.

2.4. Ultra-High Performance Liquid Chromatography—High Resolution Mass Spectrometry (UHPLC–HRMS) Metabolomics Analysis

UHPLC–HRMS analysis has been described previously [48,49]. Briefly, metabolites were separated on a Dionex UltiMate 3000 RS (Sunnyvale, CA, USA) by injecting a 10 µL sample on a Synergy reverse phase Hydro-RP 100 Å, 100 mm × 2.00 mm, 2.5 µm pore size LC column (Phenomenex, Torrance, CA, USA) kept at 25 °C. The global metabolomics method, adapted from [50], ran for 26 min with the application of a multistep gradient. To separate the analytes, two HPLC-grade solvents were used in gradient steps. Solvent A (97:3 H₂O:MeOH with 11 mM tributylamine and 15 mM acetic acid) and solvent B (100% MeOH). The gradient was performed as follows: 0 min, 0% B; 5 min, 20% B; 13 min, 55% B; 15.5 min, 95% B; 19 min, 0% B; 25 min, 0% B with a flow rate of 200 µL/min. The eluent was administered into the mass spectrometer via an electrospray ionization (ESI) source conjoined to an Exactive™ Plus Orbitrap Mass Spectrometer (Thermo Scientific, Waltham, MA, USA) under the following established parameters of aux gas: 8; sheath gas: 25; sweep gas: 3; spray voltage: 3.00 kV; and capillary temperature: 300 °C. The parameters of the mass spectrometer were set as follows: resolution: 140,000; automatic gain control (AGC): 3 × 10⁶; maximum IT time: 100; scan range: 85–1000 *m/z*. Raw data were obtained from the Xcalibur MS software (Thermo Electron Corp, Waltham, MA, USA) and converted to mzML format by ProteoWizard tool MSConverter [51,52]. The converted data were analyzed using MAVEN [53], and peaks were annotated with a maximum allowed error of 5 ppm. Area under the chromatographic curve was integrated based upon an in-house verified list of metabolites using exact mass and known retention times [54]. All metabolite

values were normalized based on the mass of the duodenum tissue extracted prior to all statistical calculations.

2.5. Ingenuity Pathway Analysis (IPA)

The metabolites' information (fold change and *p*-value) as well as their IDs (Human Metabolome Database, HMDB [55]; Kyoto Encyclopedia of Genes and Genomes, KEGG [56]; and Chemical Entities of Biological Interest, ChEBI [57]) were introduced for the IPA analysis to determine the canonical pathways, functional annotation, upstream and downstream analysis, and molecular network discovery using a cut-off of FDR adjusted *p*-value < 0.05 and a fold change between −1.5 and 1.5.

2.6. RNA Isolation and Quantitative Real-Time PCR

Isolation, integrity assessment, and concentration measurement of duodenal total RNA were previously described [58–61]. Duodenal total RNA samples were DNase treated, reverse-transcribed using qScript cDNA Synthesis Supermix (Quanta Biosciences, Gaithersburg, MD, USA), and amplified by real-time quantitative PCR (Applied Biosystems 7500 Real Time System) with PowerUp SYBR green master mix (Life Technologies, Carlsbad, CA, USA) as previously described [58–61]. The qPCR cycling conditions and melt curve analysis were previously reported [58–61]. Relative expression of the target genes was determined using the $2^{-\Delta\Delta CT}$ method, with normalization to 18s rRNA as a house-keeping gene [62]. Oligonucleotide primer sequences specific for chicken are presented in Table 1.

Table 1. Oligonucleotide real-time qPCR primers.

Gene	Accession Number ^a	Primer Sequence (5'→3')	Orientation	Product Size (bp)
CA9	XM_004937157	GGGATGTGCTTGCTGTGCTAT	Forward	58
		AGGAAAGCCAGCATTGTGATG	Reverse	
HDAC11	NM_001277141	ACCAGTCCTCTTTCTTCCCAACT	Forward	63
		GGGTTTCGAGAGGTTTCAAA	Reverse	
CPT1	AY675193	GCCCTGATGCCTTCATTCAA	Forward	60
		ATTTTCCCATGTCTCGGTAGTGA	Reverse	
MAPK3	NM_204150	CGGACCATGATCACACAGGAT	Forward	63
		CAGGAGCCCTGTACCAACGT	Reverse	
MAPK1	AY033635	CGGACCATGATCACACAGGAT	Forward	63
		CAGGAGCCCTGTACCAACGT	Reverse	
MAPK14	XM_419263	AGCTGGAGATTGAGGAATGGAA	Forward	62
		CGGTGGCACAAGCTGATTA	Reverse	
MAPK9	NM_205095	GCCGATGATCAGCCAGGAT	Forward	62
		GGCCCAATGGAAGCAAGAG	Reverse	
SOD1	NM_205064	TGGCTTCCATGTGCATGAAT	Forward	58
		AGCACCTGCGCTGGTACAC	Reverse	
SOD2	NM_204211	GCTGGAGCCCCACATCAGT	Forward	61
		GGTGGCGTGGTGTGTTGCT	Reverse	
18S	AF173612	TCCCCTCCCCTTACTTGGAT	Forward	60
		GCGCTCGTCGGCATGTA	Reverse	

^a Accession numbers refer to Genbank (NCBI). CA9, carbonic anhydrase 9; HDAC 11, histone deacetylase 11; MAPK, mitogen-activated protein kinase; SOD, superoxide dismutase.

2.7. Immunoblot Analysis

Duodenal tissue homogenization, protein isolation, and protein concentration measurement using Bradford assay and Synergy HT multimode microplate reader (BioTek, Winooski, VT, USA) were previously described [63]. Proteins (80 µg) were run on 4–12% gradient Bis–Tris gels (Life Technologies, Carlsbad, CA, USA) and transferred to PVDF membranes. The membranes were blocked with 5% non-fat milk in tris-buffered saline with Tween 20 detergent (TBS-T) for 1 h at room temperature, then incubated with primary antibodies (1:500–1:1000 dilution) overnight at 4 °C. Secondary antibodies (1:5000)

were diluted in 5% milk in TBS-T, and membranes were incubated at room temperature for 1 h. Primary antibodies used were: rabbit anti-phospho-ERK1/2^{Thr202/Tyr204}, rabbit anti-ERK1/2, rabbit anti-phospho-P38 MAPK^{Thr180/Tyr182}, rabbit anti-P38 MAPK (Cell Signaling Technology, Danvers, MA, USA), and rabbit anti-GAPDH antibody (Santa Cruz Biotechnology, Dallas, TX, USA) as a housekeeping protein to assess protein loading. After another wash, secondary anti-rabbit IgG and HRP-linked antibody (Cell Signaling Technology, Danvers, MA) diluted to 1:5000 were added to 5% nonfat milk in TBS and Tween 20 and incubated with the membranes at room temperature for 1 h. The signal was visualized by chemiluminescence (ECL Plus, GE Healthcare, Pittsburg, PA, USA) and captured by the FluorChem M MultiFluor System (ProteinSimple, San Jose, CA, USA).

2.8. Data Processing and Statistical Analysis

Original datasets from all studied groups have been submitted to EMBL-EBI MetaboLights database, DOI: 10.1093/nar/gkz1019, PMID:31691833) with the identifier MTBLS4513 (<https://www.ebi.ac.uk/metabolights/MTBLS4513>) (access on 20 March 2022). Metabolites showing differences higher or lower than 1.5 folds and *p*-value less than 0.05 in the comparison between each of the treatment groups (AHS, PHS, CHS, and PF) and TN (control) birds were considered differentially abundant. Heat maps, which displayed log₂ fold changes for identified metabolites, were created with Cluster 3.0 [64] and Javaview 1.1 [65]. *p*-values were calculated using Student's *t*-test or Student–Newman–Keuls (SNK) method as appropriate. For group discrimination, partial least squares discriminant analysis (PLS-DA) and variable importance in projection (VIP) scores were constructed using the MetaboAnalyst 5 [66] and statistical package Discriminer in R version 3.6.1 (<https://cran.r-project.org>) (access on 20 March 2022). Metabolites with VIP values > 1 were the ones that contributed to the group differentiation, and this was considered as a significant VIP score.

3. Results

3.1. Global Analysis of the Duodenal Dynamic Metabolic Profiling

The global metabolomics profiling analyses identified a total of 218 metabolites with 178 that were highly abundant, while 40 were not detectable in broiler duodenum. The heat map provides a general overview of the identified metabolite relative abundances for each treatment group compared to TN group (Figure 2).

The 178 identified metabolites have been submitted to MetaboLights database (<https://www.ebi.ac.uk/metabolights>) (access on 20 March 2022) and are presented in Table S1. As depicted in Figure 3, the only treatment with clear separation from the TN group in the 2D PLS-DA plot was the CHS group (Figure 3g). However, the 3D PLS-DA plots showed clear separation between TN and each of the PHS (Figure 3b), PF (Figure 3d), AHS (Figure 3f), and CHS (Figure 3h) groups.

When all of the groups were plotted together, the segregation was less clear (data not shown). In order to determine which metabolites drove the separation between the groups, each metabolite was assigned a VIP score representing its importance to the PLS-DA model with a VIP score >1 reflecting a significant influence on the separated clusters observed. As shown by the VIP score plot, the 15 metabolites with the highest VIP scores were identified for each comparison (Figure 4a–d).

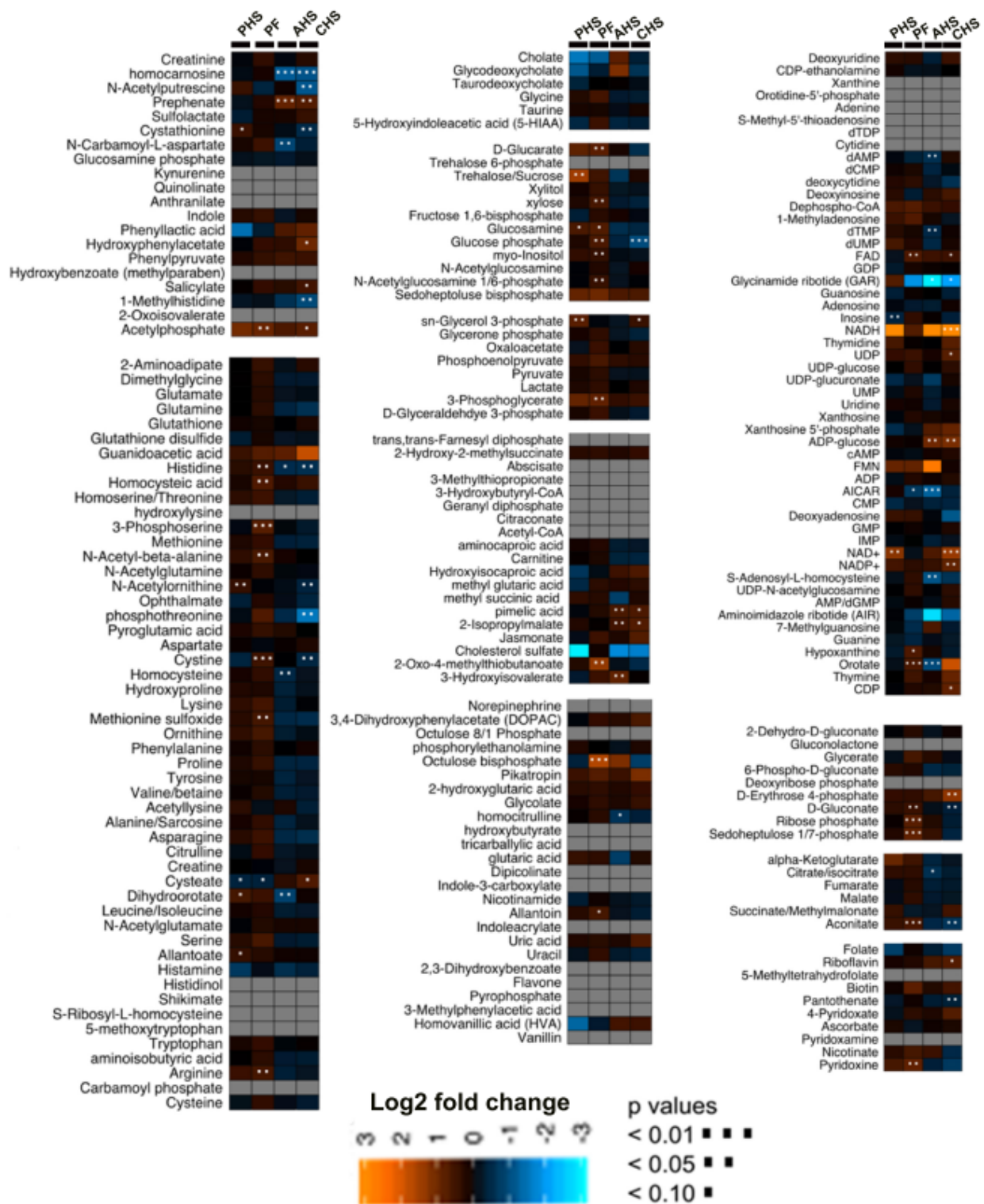


Figure 2. Heat map of relative levels of broiler duodenal metabolites modulated by heat stress exposure. Heat map was built using log2 fold change and VIP score and by comparing each treatment (PHS, AHS, CHS, and PF) to the TN group. AHS, acute heat stress; CHS, chronic heat stress; PF, pair fed; PHS, pre-heat stress group. The empty cells indicate that the metabolites were not detected.

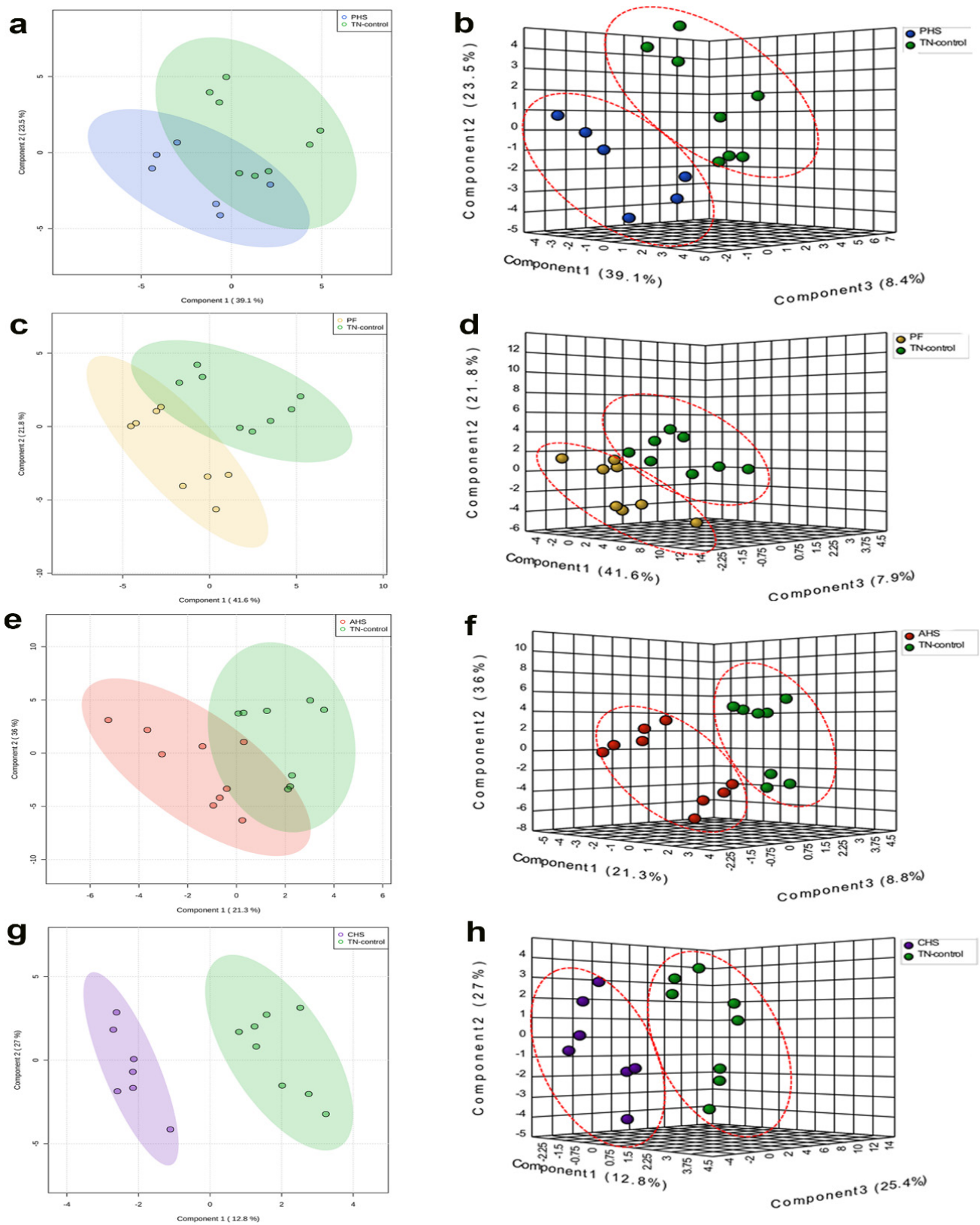


Figure 3. Partial least squares-discriminant analysis (PLS-DA) 2D and 3D score plots. PLS-DA was constructed using the statistical package DiscrMiner in R version 3.6.1 and displayed different clusters when comparing metabolite profiles between TN and treated (CHS, AHS, PF, and PHS) birds (a,c,e,g). AHS (f), acute heat stress; CHS (h), chronic heat stress; PF (d), pair fed; PHS (b), preheat stress; TN, thermoneutral.

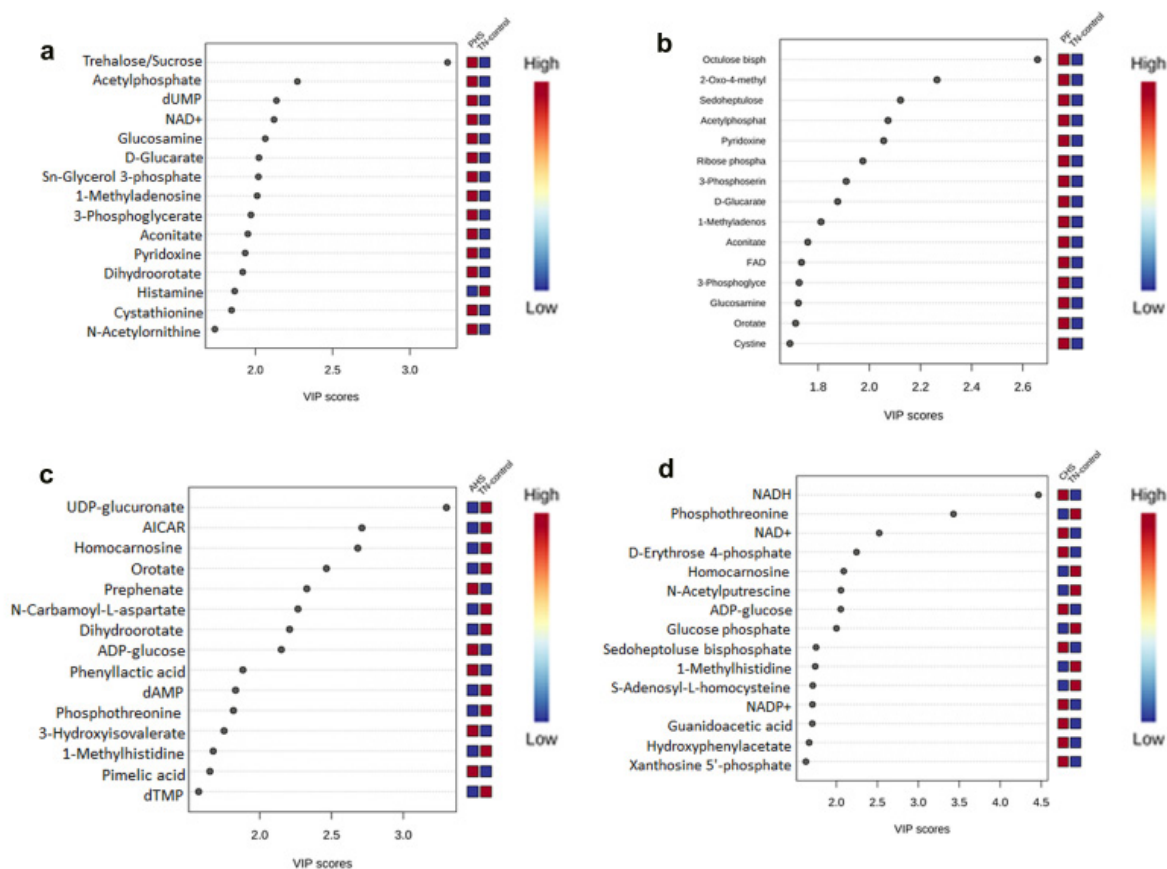


Figure 4. VIP scores and related concentrations of the differentially abundant metabolites. Top 15 metabolites based on VIP scores from PLS-DA analysis comparing TN to PHS (a), TN to PF (b), TN to AHS (c), and TN to CHS (d). AHS, acute heat stress; AICAR, 5-aminoimidazole-4-carboxamide-1- β -D-ribofuranoside; CHS, chronic heat stress; dAMP, deoxyadenosine monophosphate; dTMP, deoxythymidine monophosphate; dUMP, deoxyuridine monophosphate; NAD⁺, nicotinamide adenine dinucleotide; NADH, reduced nicotinamide adenine dinucleotide; PHS, preheat stress; PF, pair fed; TN, thermoneutral.

3.2. Identification of Potential Metabolic Signatures

For more stringent analyses, metabolites with the greatest discriminating potential between the thermoneutral (TN) and each of the treated-groups (PHS, PF, AHS, or CHS) were assessed by unpaired *t*-test with significance level $p < 0.05$. As shown in Table 2, metabolites were clustered in a group-specific manner. For instance, cystathionine, N-acetylmethionine, dihydroorotate, allantoate, and trehalose were specifically and significantly abundant in the duodenum of PHS group (Table 2). Acetylphosphate, histidine, homocysteic acid, 3-Phosphoserine, N-Acetyl-beta-alanine, cystine, methionine sulfoxide, arginine, D-glucarate, xylose, glucose phosphate, myo-inositol, N-acetylglucosamine 1/6-phosphate, 3-Phosphoglycerate, 2-oxo-4-methylthiobutanoate, hypoxanthine, orotate, octulose bisphosphate, allantoin, D-gluconate, ribose phosphate, sedoheptulose 1/7-phosphate, aconitate, and pyridoxine were significantly high in the duodenum of the PF group (Table 2). 3-Hydroxyisovalerate was specifically high in the AHS group only; however, hydroxyphenylacetate, salicylate, NADH, UDP, NADP⁺, CDP, D-erythrose 4-phosphate, and riboflavin were abundant in the duodenum of the CHS group (Table 2). On the other hand, inosine was significantly decreased in PHS duodenum; however, N-carbamoyl-L-aspartate, homocysteine, dAMP, dTMP, S-adenosyl-L-homocysteine, homocitrulline, and citrate were significantly low in the duodenum of the AHS group (Table 2). N-acetylputrescine, 1-methylhistidine, phosphothreonine, and pantothenate were specifically depressed in the duodenum of the CHS group (Table 2).

Table 2. Potential duodenal metabolic biomarkers ¹.

	HMDB ID	PHS	PF	AHS	CHS
Cystathionine	HMDB0000099	+			-
N-Acetylornithine	HMDB0003357	+			-
Dihydroorotate	HMDB0003349	+		-	
Allantoate	HMDB0001209	+			
Trehalose	HMDB0000975	+			
Glucosamine	HMDB0001514	+	+		
sn-Glycerol 3-phosphate	HMDB0000126	+			+
NAD+	HMDB0000902	+			+
Cysteate	HMDB0002757	-	-		+
Inosine	HMDB0000195	-			
Acetylphosphate	HMDB0001494		+		+
Histidine	HMDB0000177		+	-	-
Homocysteic acid	HMDB0002205		+		
3-Phosphoserine	HMDB0000272		+		
N-Acetyl-beta-alanine	HMDB0061880		+		
Cystine	HMDB0000192		+		-
Methionine sulfoxide	HMDB0002005		+		
Arginine	HMDB0000517		+		
D-glucarate	HMDB0000663		+		
Xylose	HMDB0000098		+		
Glucose phosphate	HMDB0001254		+		-
Myo-inositol	HMDB0000211		+		
N-Acetylglucosamine 1/6-phosphate	HMDB0002817		+		
3-Phosphoglycerate	HMDB0000807		+		
2-Oxo-4-methylthiobutanoate	HMDB0001553		+		
FAD	HMDB0001248		+		+
Hypoxanthine	HMDB0000157		+		
Orotate	HMDB0000226		+	-	
Octulose bisphosphate	N/A		+		
Allantoin	HMDB0000462		+		
D-gluconate	HMDB0000625		+		-
Ribose phosphate	HMDB0001548		+		
Sedoheptulose 1/7-phosphate	HMDB0060509		+		
Aconitate	HMDB0000072		+		-
Pyridoxine	HMDB0000239		+		
AICAR	HMDB0001517		-		
Prephenate	HMDB0012283			+	+
pimelic acid	HMDB0000857			+	+
2-Isopropylmalate	HMDB0000402			+	+
3-Hydroxyisovalerate	HMDB0000754			+	
ADP-glucose	HMDB0006557			+	+
Homocarnosine	HMDB0000745			-	-
N-Carbamoyl-L-aspartate	HMDB0000828			-	
Homocysteine	HMDB0000742			-	
dAMP	HMDB0000905			-	
dTMP	HMDB0001227			-	
Glycinamide ribotide (GAR)	HMDB0002022			-	-
S-Adenosyl-L-homocysteine	HMDB0000939			-	
Homocitrulline	HMDB0000679			-	
Citrate/isocitrate	HMDB0000193			-	
Hydroxyphenylacetate	HMDB0000020				+
Salicylate	HMDB0000500				+
NADH	HMDB0001487				+
UDP	HMDB0000295				+
NADP+	HMDB0000217				+
CDP	HMDB0001546				+
D-Erythrose 4-phosphate	HMDB0001321				+
Riboflavin	HMDB0000244				+
N-Acetylputrescine	HMDB0002064				-
1-Methylhistidine	HMDB0000001				-
Phosphothreonine	HMDB0011185				-
Pantothenate	HMDB0000210				-

¹ AHS, acute heat stress; CHS, chronic heat stress; HMDB, human metabolome database; PHS, preheat stress; PF, pair fed; +, increase; -, decrease.

It is worth noting that the levels of some duodenal metabolites followed opposite patterns between groups. For example, cystathionine was abundant in the PHS group but depressed in the CHS group (Table 2). Dihydroorotate was high in the PHS but low in the AHS group. Cysteate was decreased in PHS and PF but increased in the CHS group (Table 2). Histidine was high in the PF but low in the AHS and CHS groups. Cystine, glucose phosphate, and D-gluconate were increased in the PF but decreased in the CHS group. Orotate was increased in the PF but decreased in the AHS group (Table 2). The differential abundance of these metabolites indicated a specific and distinct metabolic pattern between TN and treated groups, and within treated groups.

3.3. Metabolic Pathway and Network Analysis

3.3.1. Top Canonical Pathways

To gain biologically related molecule networks, the above identified metabolites (172 from 178) were mapped into the IPA knowledge-base and analyzed to outline the most enriched biological functions. Using a cut-off of FDR adjusted p -value <0.05 and a fold-change between -0.5 and 0.5 , several common and specific top canonical pathways were generated (Table 3). The adenosine nucleotide degradation and dopamine degradation pathways were specific to the AHS group (Table 3). The UDP-D-xylose and UDP-D-glucuronate biosynthesis pathways were generated only for the CHS group (Table 3); however, the tRNA charging, pyruvate fermentation to lactate, and Glycerol-3-phosphate shuttle pathways were specific to the PHS birds. The sirtuin signaling pathway and gluconeogenesis pathway were specific to the PF group (Table 3). The pathways associated with purine nucleotide degradation, urate biosynthesis/inosine 5'-phosphate degradation, and ascorbate recycling were common for both the AHS and CHS (Table 3). The salvage pathways of pyrimidine deoxyribonucleotides were identified in both CHS and PF groups (Table 3). The glycine betaine degradation and creatine biosynthesis pathways were generated for both the PHS and PF groups (Table 3). Within the common purine nucleotide degradation pathway, hypoxanthine was specific to AHS, but adenosine and GMP were specific to the CHS group (Table 3). In the ascorbate recycling pathway, glutathione was specific to the CHS but not the AHS group (Table 3). In the salvage pathways of pyrimidine deoxyribonucleotides, deoxycytidine and uracil were specific to the PF group (Table 3). Similarly, within the creatine biosynthesis pathway, *s*-adenosylhomocysteine was specific to the PF group (Table 3).

3.3.2. Top Diseases and Disorders

The top diseases and disorders enriched by the IPA core analysis for the differentially abundant (DA) metabolites were ranked by p -value and summarized in Table 4. Cancer was a common disorder enriched with 36, 22, and 45 metabolites (molecules) in the PHS, CHS, and PF groups, respectively (Table 4). The 3-Venn diagrams showed that 33.3, 22.2, 7.4, and 5.6% of the total metabolites were common between PHS-PF, PHS-PF-CHS, PHS-CHS, and CHS-PF, respectively (Figure 5a). The metabolites AICAR and creatine were specific to PHS; 4-hydroxy-3-methoxyphenylacetic acid, adenosine, and cAMP were specific to CHS; and 5-hydroxyindol-3-acetic acid, folic acid, fructose-1,6-diphosphate, fumaric acid, glutathione disulfide, guanosine, inosine, L-cysteine, malic acid, niacinamide, ophthalmic acid, and uracil were specific to the PF group (Figure 5a). The second common disorder enriched was organismal injury, including GI abnormality, with 51, 23, 29, and 70 molecules in the PHS, AHS, CHS, and PF groups, respectively (Table 4). The 4-Venn diagrams revealed that 28, 12.2, 9.8, 3.7, 3.7, 3.7, 2.4, 2.4, 2.4, and 1.2% of the total metabolites were common between PHS-PF, PHS-PF-CHS, PHS-PF-CHS-AHS, PHS-CHS-AHS, PHS-PF-AHS, PF-AHS, PHS-CHS, PF-CHS, CHS-AHS, and PF-CHS-AHS, respectively (Figure 5b). AICAR and xylitol were specific to PHS, adenosine was distinct for CHS; however, cholic acid, glycodeoxycholic acid, and taurodeoxycholic acid were particular for the AHS group (Figure 5b). Hematological disorder was enriched in both PHS and CHS, with 13 and 8 molecules, respectively (Table 4). Venn diagrams showed that adenosine, cAMP, and oxaloacetic acid were specific to CHS; however, L-arginine, L-asparagine, L-carnitine, L-

homocysteine, L-methionine, myo-inositol, nicotinic acid, and pyridoxine were specific to the PHS group (Figure 5c).

Table 3. Top canonical pathways enriched by observed metabolite alterations in heat stress environment.

Canonical Pathways	Molecules	Treatments ¹							
		PHS		AHS		CHS		PF	
		<i>p</i> -Value	Ratio	<i>p</i> -Value	Ratio	<i>p</i> -Value	Ratio	<i>p</i> -Value	Ratio
Purine Nucleotides Degradation	Hypoxanthine *, inosine, NAD ⁺ , NADH, uric acid, xanthosine, xanthosine monophosphate, adenosine †, GMP †	-	-	7.7×10^{-8}	0.412	5.0×10^{-7}	0.412	-	-
Urate Biosynthesis/Inosine 5'-phosphate degradation	NAD ⁺ , NADH, uric acid, xanthosine, xanthosine monophosphate	-	-	1.0×10^{-6}	0.556	4.0×10^{-6}	0.556	-	-
Adenosine Nucleotides Degradation	Hypoxanthine, inosine, NAD ⁺ , NADH, uric acid	-	-	3.8×10^{-6}	0.455	-	-	-	-
Dopamine Degradation	3',5'-ADP, 3,4-dihydroxyphenylacetic, NAD ⁺ , NADH	-	-	1.5×10^{-5}	0.357	-	-	-	-
Ascorbate Recycling	Ascorbic acid, NAD ⁺ , NADH, NADP, glutathione †	-	-	2.5×10^{-5}	0.5	1.8×10^{-6}	0.625	-	-
UDP-D-xylose and UDP-D-glucuronate Biosynthesis	NAD ⁺ , NADH, UDP-D-glucose, UDP-glucuronic acid	-	-	-	-	5.5×10^{-6}	0.8	-	-
Salvage Pathways of Pyrimidine Deoxyribonucleotides	Deoxyuridine, dTMP, dUMP, thymidine, thymine, deoxycytidine †, uracil †	-	-	-	-	2.3×10^{-5}	0.417	1.6×10^{-6}	0.583
Glycine Betaine Degradation	Dimethylglycine, glycine, L-homocysteine, L-methionine, L-serine, Pyruvic acid, sarcosine	6.1×10^{-7}	0.538	-	-	-	-	3.3×10^{-6}	0.538
trRNA Charging	Glycine, L-arginine, l-asparagine, L-aspartic acid, L-histidine, L-methionine, L-phenylalanine, L-proline, l-serine, L-tryptophan, L-tyrosine	2.5×10^{-6}	0.256	-	-	-	-	-	-
Creatine Biosynthesis	Creatine, glycine, glycoamine, L-arginine, L-ornithine, S-adenosylhomocysteine †	4.3×10^{-6}	0.714	-	-	-	-	3.0×10^{-7}	0.857
Pyruvate Fermentation to Lactate	L-lactic acid, NAD ⁺ , NADH, Pyruvic acid	4.8×10^{-6}	1	-	-	-	-	-	-

¹ AHS, acute heat stress; CHS, chronic heat stress; HMDB, human metabolome database; PHS, preheat stress; PF, pair. * specific for AHS, † specific for CHS, ‡ specific for PF.

Table 4. Top diseases and disorders for DA metabolites in broiler duodenum under heat stress environment.

Diseases and Functions	Treatments ¹							
	PHS		AHS		CHS		PF	
	<i>p</i> -Value	# Mol.	<i>p</i> -Value	# Mol.	<i>p</i> -Value	# Mol.	<i>p</i> -Value	# Mol.
Cancer	4.7×10^{-2} – 8.8×10^{-9}	36	-	-	3.3×10^{-2} – 2.2×10^{-5}	22	4.9×10^{-2} – 4.7×10^{-10}	45
Organismal Injury and abnormalities	4.7×10^{-2} – 8.8×10^{-9}	51	4.9×10^{-2} – 6.5×10^{-4}	23	3.3×10^{-2} – 2.2×10^{-5}	29	4.9×10^{-2} – 4.7×10^{-10}	70
Hepatic system disease	4.7×10^{-2} – 1.7×10^{-5}	22	-	-	-	-	-	-
Hematological disease	4.7×10^{-2} – 1.3×10^{-4}	13	-	-	3.3×10^{-2} – 2.9×10^{-4}	8	-	-
Ophthalmic disease	-	-	2.5×10^{-2} – 6.5×10^{-4}	3	-	-	-	-
Cardiovascular disease	-	-	4.8×10^{-2} – 1.9×10^{-3}	3	-	-	-	-
Developmental disorders	-	-	4.2×10^{-2} – 1.9×10^{-3}	4	-	-	-	-
Hereditary disorders	-	-	4.2×10^{-2} – 1.9×10^{-3}	6	-	-	-	-
Neurological disease	-	-	-	-	3.3×10^{-2} – 1.2×10^{-4}	21	-	-
Psychological disorders	-	-	-	-	3.3×10^{-2} – 8.3×10^{-4}	15	-	-
Inflammatory disease	-	-	-	-	-	-	4.9×10^{-2} – 1.4×10^{-6}	21
Inflammatory response	-	-	-	-	-	-	4.7×10^{-2} – 1.4×10^{-6}	32

¹ AHS, acute heat stress; CHS, chronic heat stress; PHS, preheat stress; PF, pair fed.

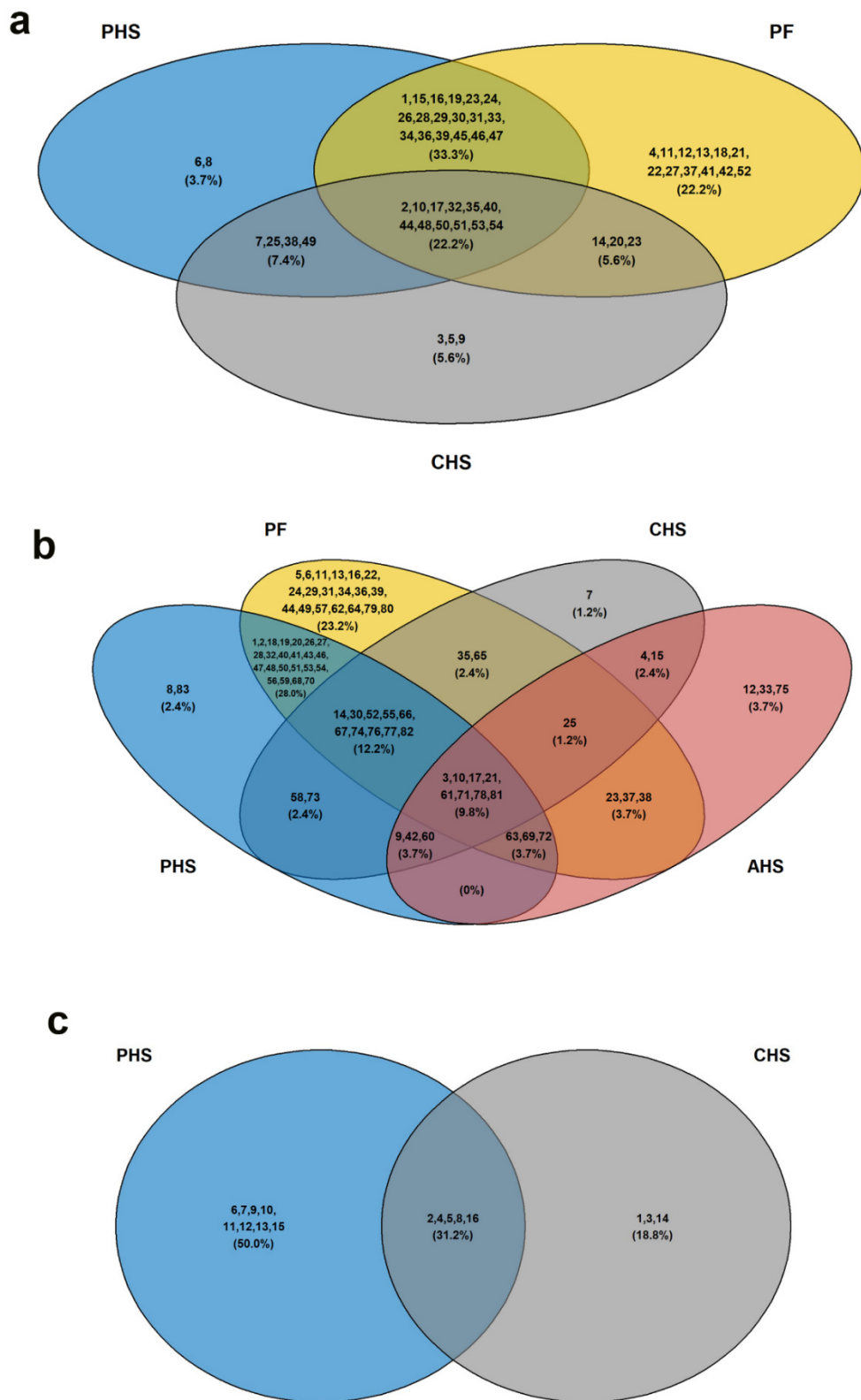


Figure 5. Venn diagrams showing the overlap of duodenal metabolites in top diseases enriched by IPA analysis. (a) Cancer, (b) organismal (GI) injury, and (c) hematological disorder. The list of the molecules is presented in Supplementary Table S1.

Hepatic system disease was enriched only in PHS with 22 molecules; ophthalmic, cardiovascular, developmental, and hereditary disorders were enriched only in AHS, with

3, 3, 4, and 6 molecules, respectively (Table 4). Neurological and psychological disorders were enriched only in CHS; however, inflammatory disease and responses were enriched in PF only (Table 4).

3.3.3. Top Molecular and Cellular Functions

The ten top molecular and cellular functions were enriched by the IPA core analysis for the DA metabolites, ranked by *p*-value, and summarized in Table 5. Amino acid metabolism and molecular transport were enriched in both PHS and PF groups (Table 5). For the amino acid metabolism, 67.6% of total metabolites were common between the PHS and PF groups; however, 20% (adenine-riboflavin dinucleotide, citrulline, folic acid, glutathione disulfide, guanosine, L-cysteine, oxalacetic acid) were specific to PF, and 11.8% (2-oxoglutaric acid, AICAR, ascorbic acid, L-aspartic acid) were particular to the PHS group (Figure 6a). For molecular transport, 58.5% of total metabolites were common between the PHS and PF groups, while 11.3% (AICAR, ascorbic acid, L-aspartic acid, N-acetylputrescine, NAD⁺, UDP) and 30.2% (citrulline, D-pantothenic acid, folic acid, glutathione disulfide, guanosine, hypoxanthine, L-cysteine, malic acid, niacinamide, orotic acid, oxalacetic acid, phosphoenolpyruvate, S-adenosylhomocysteine, UDP-D-glucose, UMP, uridine) were specific to PHS and PF, respectively (Figure 6b).

Table 5. Top molecular and cellular functions for DA metabolites in broiler duodenum under heat stress environment.

Molecular and Cellular Functions	PHS		AHS		Treatments ¹		PF				
	<i>p</i> -Value	# Mol.	<i>p</i> -Value	# Mol.	CHS <i>p</i> -Value	# Mol.	<i>p</i> -Value	# Mol.			
Amino acid metabolism	4.7×10^{-2}	1.1×10^{-8}	27	-	-	-	4.9×10^{-2}	8.9×10^{-9}	31		
Molecular transport	4.7×10^{-2}	1.1×10^{-8}	37	-	-	-	4.9×10^{-2}	2.5×10^{-8}	48		
Small molecule biochemistry	4.7×10^{-2}	1.1×10^{-8}	44	4.6×10^{-2}	8.4×10^{-5}	28	-	4.9×10^{-2}	2.5×10^{-8}	58	
Protein synthesis	2.6×10^{-2}	1.7×10^{-7}	18	-	-	3.3×10^{-2}	2.0×10^{-4}	11	1.4×10^{-2}	3.6×10^{-7}	22
Cell death and survival	4.7×10^{-2}	7.5×10^{-7}	36	-	-	3.3×10^{-2}	1.2×10^{-4}	26	-	-	
Nucleic acid metabolism	-	-	-	4.5×10^{-2}	1.8×10^{-5}	21	-	-	-	-	
DNA replication, damage, and repair	-	-	-	4.2×10^{-2}	3.0×10^{-4}	11	-	-	-	-	
Energy production	-	-	-	4.2×10^{-2}	3.0×10^{-4}	12	-	-	-	-	
Carbohydrate metabolism	-	-	-	4.3×10^{-2}	6.5×10^{-4}	10	-	-	-	-	
Free radical scavenging	-	-	-	-	-	3.3×10^{-2}	1.4×10^{-4}	12	-	-	

¹ AHS, acute heat stress; CHS, chronic heat stress; PHS, preheat stress; PF, pair fed.

Small molecule biochemistry was enriched in PHS, AHS, and PF with 44, 28, and 58 molecules, respectively (Table 5). As shown by Venn diagram, 37.5%, 13.9%, 8.3%, and 6.9% were common between PHS-PF, PHS-PF-AHS, AHS-PF, and PHS-AHS, respectively (Figure 6c). The group-specific enriched metabolites were AICAR and N-acetylputrescine for PHS, cholic acid, cAMP, glycodeoxycholic acid, L-cysteic acid, L-homocysteic acid, taurodeoxycholic acid, UDP-D-glucose for AHS, and citrulline, folic acid, glutathione disulfide, guanosine, homocarnosine, L-cysteine, L-cystine, malic acid, niacinamide, orotic acid, oxalacetic acid, S-adenosylhomocysteine, UDP-N-acetylglucosamine, UMP, and uridine for the PF group (Figure 6c).

Protein synthesis was enriched in PHS, CHS, and PF groups with 18, 11, and 22 molecules, respectively (Table 5). As shown in Figure 6d, the Venn diagram revealed that L-alpha-hydroxyisocaproic acid was specific to the CHS group; however, cholesterol sulfate, citrulline, L-cysteine, L-cystine, niacinamide, and taurine were specific to the PF group.

Cell death and survival was enriched in both the PHS and CHS groups, with 36 and 26 molecules, respectively (Table 5). Venn diagram showed that 3,4-dihydroxyphenylacetic acid, adenosine, cAMP, orotic acid, oxalacetic acid, and UDP-D-glucose were specific to the CHS group; however, 2-deoxyadenosine, 2-oxoglutaric acid, AICAR, deoxycytidine, glucosamine, glycine, L-arginine, L-asparagine, L-carnitine, L-histidine, L-methionine, L-proline, L-serine, L-tyrosine, pyridoxine, and pyruvic acid were specific to the PHS group (Figure 6e).

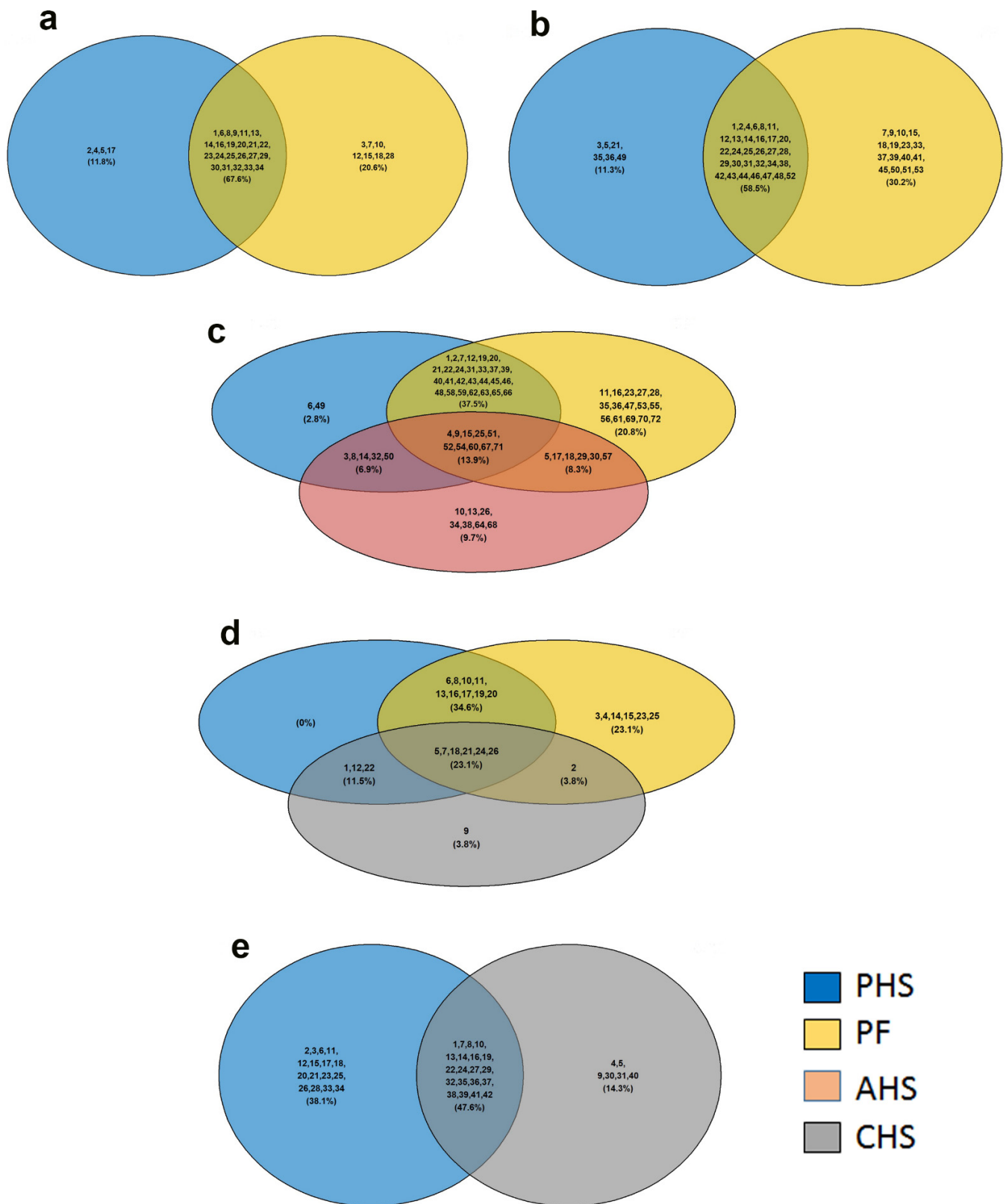


Figure 6. Venn diagrams showing the overlap of duodenal metabolites in top molecular and cellular functions enriched by IPA analysis. (a) Amino acid metabolism, (b) molecular transport, (c) small molecule biochemistry, (d) protein synthesis, and (e) cell death and survival. The list of the molecules is presented in supplementary Table S1 AHS, acute heat stress; CHS, chronic heat stress; PHS, preheat stress; PF, pair fed.

Nucleic acid metabolism, DNA replication, damage, and repair, energy production, and carbohydrate metabolism were enriched in the AHS group; however, free radical production and scavenging was refined in the CHS group (Table 5).

3.3.4. Top Up- and Downstream Regulators

To mine the duodenal metabolome data further, we next assessed how the DA metabolites interacted with intracellular or transcellular signaling and molecules. The integrated IPA-predicted upstream regulators are summarized in Table 6. In the PHS group, glycine N-methyl transferase (GNMT) and carnitine palmitoyltransferase 1B (CPT1B) were inhibited, while histone deacetylase 11 (HDAC11), carbonic anhydrase 9 (CA9), GATA binding protein 4, and matrix metalloproteinase 11 (MMP11) were activated. In CHS birds, CPT1B and IL37 were predicted to be inhibited; however, CA9 was activated. In the AHS group, both CPT1B and cystathionine gamma-lyase (CTH) were predicted to be inhibited. In the PF group, GNMT, IL37, and CPT1B were projected to be inhibited, and CA9, GATA4, and HDAC11 were activated (Table 6). We extended the IPA analyses to predict the downstream mediators, and as shown in Figure 7, the causal network indicated that MAPK and mitochondrial enzymes were central subsequent mediators. The extracellular signal-related kinase 1/2 (ERK1/2) was a central hub for all of the tested groups (Figure 7a–d). The mitochondrial superoxide dismutase (SOD) and cytochrome C oxidase were scored in both the PHS and CHS birds. The mitochondrial succinate dehydrogenase was inferred in the PHS and PF groups. The mitochondrial NDP kinase was predicted in the PF and AHS birds.

Table 6. Top upstream regulators for DA metabolites in broiler duodenum under heat stress environment.

Upstream Regulators ²	Treatments ¹							
	PHS		AHS		CHS		PF	
	<i>p</i> -Value	Z Score	<i>p</i> -Value	Z Score	<i>p</i> -Value	Z Score	<i>p</i> -Value	Z Score
GNMT	4.1×10^{-4}	−2.23	-	-	-	-	8.0×10^{-7}	−2.82
CPT1B	1.9×10^{-9}	−2.49	1.3×10^{-4}	−2.44	1.1×10^{-5}	−2.82	1.9×10^{-17}	−3.71
GATA4	2.8×10^{-6}	2.82	-	-	-	-	1.8×10^{-4}	2.64
MMP11	2.2×10^{-5}	2.00	-	-	-	-	-	-
IL37	-	-	-	-	9.9×10^{-4}	−2.23	2.9×10^{-10}	−2.49
CA9	1.5×10^{-11}	3.31	-	-	1.6×10^{-3}	2.00	6.9×10^{-9}	3.16
HDAC11	2.1×10^{-4}	2.00	-	-	-	-	5.9×10^{-4}	2.0
CTH			7.9×10^{-5}	−2.0	-	-	-	-

¹ AHS, acute heat stress; CHS, chronic heat stress; PHS, preheat stress; PF, pair fed; ² CA9, Carbonic anhydrase; CPT1B, Carnitine palmitoyltransferase 1B; CTH, Cystathionine gamma-lyase; GATA4, GATA binding protein 4; GNMT, glycine N-methyltransferase; HDAC11, histone deacetylase 11; IL37, interleukin 37; MMP11, matrix metalloproteinase 11.

The mitochondrial complex I was found in the PHS group. At the nuclear level, the activator protein 1 (AP-1) and UDP-glucuronosyltransferase (UGT) were mapped in AHS and CHS, respectively. QPCR analyses of a few selected genes showed that the duodenal expression of *CA9* and *HDAC11* was downregulated in the CHS and AHS group, and *CPT1* in the PF and PHS birds (Figure 8a–c). The expression of duodenal *MAPK14* (P38 MAPK), *MAPK9* (JNK2), and *SOD1* was downregulated in the CHS and PHS groups compared to the TN birds (Figure 8f,h). The expression of *MAPK1* (ERK2) and *SOD2* was downregulated in the CHS compared to TN group (Figure 8e,i); however, the *MAPK3* (ERK1) mRNA abundances remained unchanged between all studied groups (Figure 8d). Western blot analysis, on the other hand, showed that the phosphorylated levels of ERK1/2 at the Thr202/Tyr204 site was significantly induced in PF but decreased in the CHS group compared to TN birds (Figure 8j,k); however, p-P38^{Thr180/Tyr182} did not differ between all groups (Figure 8j,l).

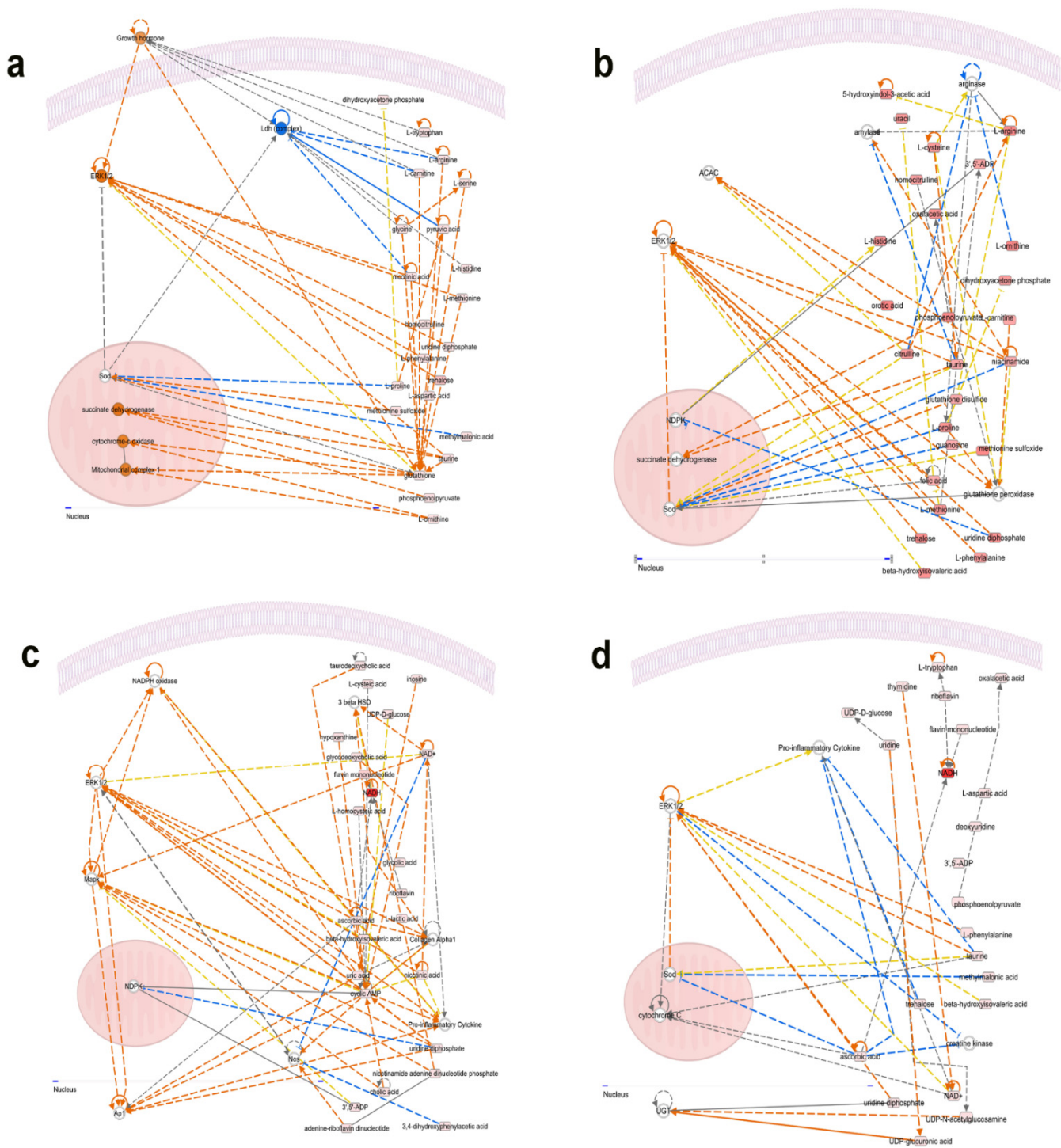


Figure 7. Predicted causal networks and downstream mediators built with IPA program from duodenal metabolomics data. (a) PHS group, (b) PF group, (c) AHS group, and (d) CHS group. AHS, acute heat stress; AP1, activator protein 1; CHS, chronic heat stress; ERK, extracellular signal-regulated kinase; MAPK, mitogen-activated protein kinase; NDPK, nucleoside diphosphate kinase; PF, pair fed; PHS, preheat stress; SOD, superoxide dismutase; UGT, UDP-glucuronosyltransferase.

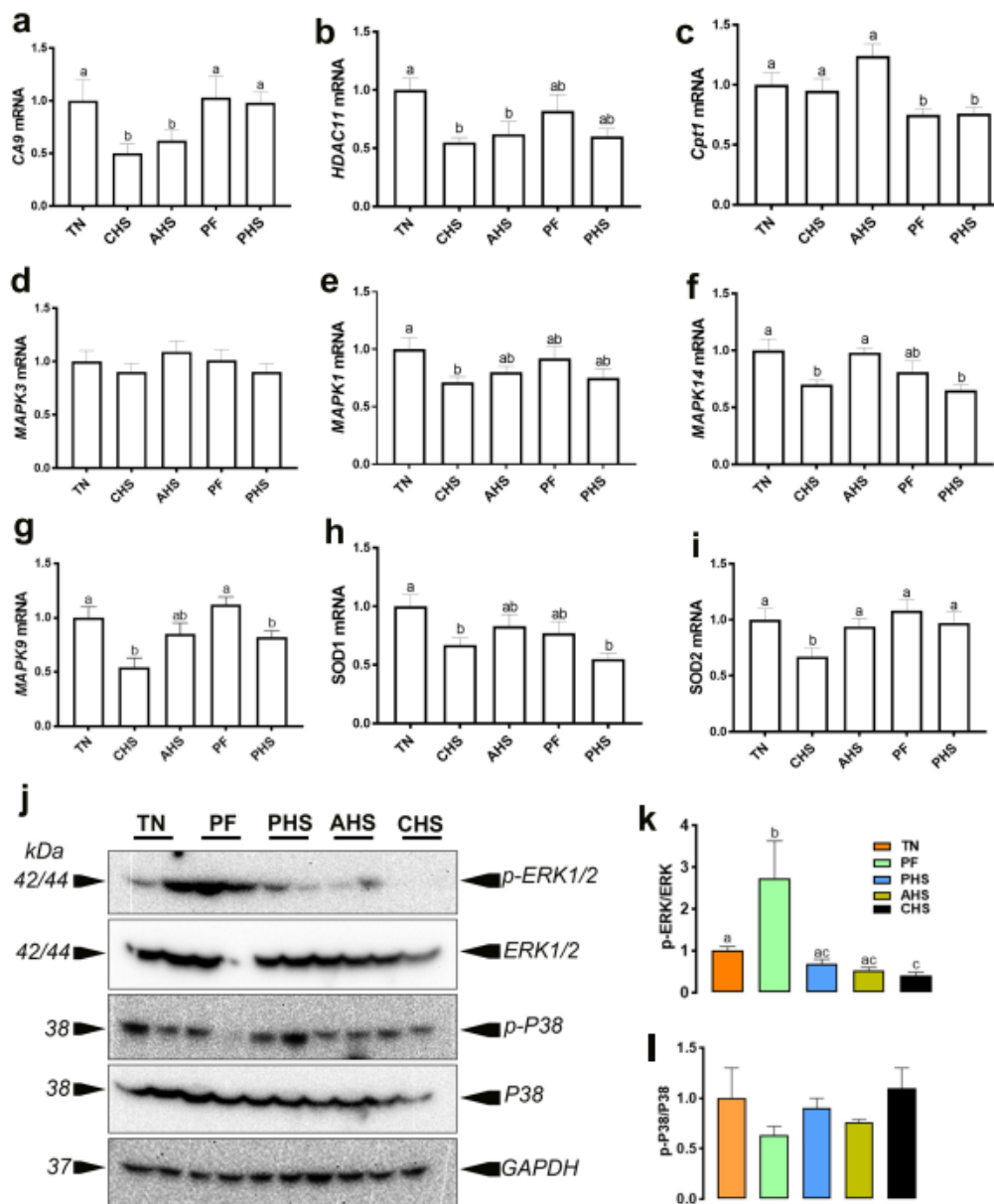


Figure 8. Effect of heat stress on the expression of SOD and MAPKs. The mRNA levels of CA9 (a), HDAC11 (b), Cpt1 (c), MAPK3 (d), MAPK1 (e), MAPK14 (f), MAPK9 (g), SOD1 (h), and SOD2 (i) were measured by real-time qPCR and $2^{-\Delta\Delta C_t}$ method [62]. The protein levels were determined by Western blot (j), and the relative expression was presented as phospho protein/ pan protein ratios (k,l). Data are presented as mean \pm SEM ($n = 8$ and 4 /group for qPCR and Western blot, respectively). Different letters are significantly different ($p < 0.05$). AHS, acute heat stress; CA9, carbonic anhydrase 9; CHS, chronic heat stress; CPT, Carnitine palmitoyltransferase; GAPDH, glyceraldehyde-3-phosphate dehydrogenase; HDAC 11, histone deacetylase 11; ERK, extracellular signal-regulated protein kinase; MAPK, mitogen-activated protein kinase; PF, pair fed; PHS, preheat stress; SOD, superoxide dismutase.

4. Discussion

High environmental heat load is one of the most challenging stressors and a stumbling block to the poultry industry as it disrupts production sustainability and inflicts heavy economic burdens worldwide [7,67]. In addition to its strong adverse effects on appetite, growth, performance, welfare, and meat quality [15–18,68], heat stress can damage body

systems and organs [69–71]. Although the underlying molecular mechanisms are not fully defined, one of the prominent effects of heat stress is gut injury [28,35,36,72]. As a continuation of our previous researches showing that heat stress alters the expression of intestinal heat-shock proteins, cyto(chemo)kines, tight junction proteins, and nutrient transporters, and thereby induces leaky gut syndrome [15,46,47], we undertook the present study to determine the duodenal metabolic profiles in heat-stressed broilers.

Due to its high resolution and sensitivity, UHPLC–HRMS-based metabolomics has become the leading means of systems biology research and has been extensively used in the biomedical, pharmaceutical, and toxicological fields [73], but its implementation is not prominent in livestock and poultry research. To our knowledge, this is the first study to explore the chemical constituents and to systematically identify DA metabolites in the duodenum of heat-stressed broilers. The results showed that heat stress exposure induced significant changes in the broiler duodenal metabolome independently of feed depression, as the PF group exhibited very minimal overlap with the AHS group and a complete separation from the CHS group. This validates that exposure to heat stress rather than differences in feed intake lead to the different metabolic profiles. Specifically, prephenate, pimelic acid, 2-isopropylmalate, and ADP-glucose were found to be significantly higher in the duodenum of both AHS and CHS birds compared to TN birds. Prephenate is involved in aromatic amino acid biosynthesis and the shikimate pathway, which is present in bacteria, fungi, plants, some parasitic protozoans, and algae, but not in animals [74,75]. Similarly, pimelic acid, also known as heptanedioic acid, is synthesized in many bacteria and is involved in the biosynthesis of lysine and biotin [76]. 2-Isopropylmalate is involved in the leucine biosynthesis pathway, which is common to prokaryotes, plants, and fungi, but absent from human and animals [77,78]. ADP-glucose, however, exists in all living organisms, ranging from bacteria to humans, and is involved in the ticlopidine metabolic pathway. These data suggest that prephenate, pimelic acid, and 2-isopropylmalate are probably microbiota-generated metabolites; however, ADP-glucose could be either microbiota- or host-derived. Although the exact identity of the bacterial/microorganism sources and species is not known at this time, it seems that heat stress modifies the intestinal microbiota- and host-dependent derivative metabolites that potentially play roles as important physiological modulators in stress responses, whether associated with dysbiosis and leaky gut or thermo-memory and adaptation [79,80].

It is worth noting that within heat stress groups and independently of feed intake reduction, there was separation based on heat stress duration, with AHS overlapping with PF, PHS, TN, and CHS, while CHS only showed overlap with AHS in the 3D PLS-DA. This demonstrates that the increased duration of HS further modulates the duodenal metabolome. In fact, 3-hydroxyisovalerate was higher only in the AHS group; however, hydroxyphenylacetate, salicylate, NADH, UDP, NADP⁺, CDP, D-erythrose 4-phosphate, and riboflavin were elevated in CHS birds. 3-Hydroxyisovalerate is a byproduct of the leucine degradation pathway and is a host-derived mitochondrial metabolite through the action of the biotin-dependent enzyme methylcrotonyl-CoA carboxylase [81]. Its high level was associated with mitochondria toxicity, redox dyshomeostasis, aciduria, and ketogenesis disorders [82,83], most of which are induced by acute heat stress [84,85]. The CHS-associated metabolites were both microbiota- and host-derived. Hydroxyphenylacetate has been shown to have a protective ability via induction of antioxidant enzyme activities in mice [86]. Salicylate was found to be central to the defense mechanism in plants [87]. In animals, salicylate inhibits cyclooxygenase-2 transcription, which has been shown to be associated with stress [88–90], including heat load [91]. In addition to mitochondrial origin, the observed high levels of NADP⁺, which were in agreement with previous studies [92], suggest that CHS induced reactive oxygen species (ROS) via the nicotinamide adenine dinucleotide phosphate oxidase pathway [92] that converts NADPH to NADP⁺ [93]. NADP⁺ can also be generated from phosphorylated NAD⁺ by the action of NAD⁺ kinases (NNT and NADKs). NADH is a central hydride donor that drives the mitochondrial oxidative phosphorylation (OXPHOS) for ATP generation along with ROS

production [94] and the conversion of lactic acid to pyruvate. Although it is not known what subcellular compartment (cytosol, mitochondria, or both) is involved, the high level of NADH supports the abovementioned hypothesis and indicates that CHS might affect the ATP level and glycerol-3-phosphate shuttles, which are a crossroad of glycolysis, fatty acid metabolism, and OXPHOS [95–98]. Furthermore, NADH can be reduced from NAD⁺ in the metabolic processes including glycolysis, β -oxidation, and the TCA cycle. Beyond its crucial role as a coenzyme in energy metabolism [99], NAD⁺ has been shown in recent years to play a vital role in stress resistance, DNA repair, cell death, and signal transduction [100–103]. Collectively, these data indicate that the increased levels of salicylate and the golden NAD⁺/NADH nucleotides may play a key role in broiler acclimatization and/or metabolic efficiency during CHS [104–108]. In addition to the abovementioned changes, CHS seemed to enhance endogenous duodenal UDP and CDP concentrations, indicating a modulation of nucleoside metabolism and duodenal intracellular uridine- and cytidine-homeostasis, which is in accordance with previous studies [109,110]. We interpret the increase in these nucleosides under our experimental conditions as an indication of metabolic shift and reprogramming to promote the use of nucleic acid precursors, likely via salvage pathway, to favor the pentose phosphate pathway (PPP) and counteract ROS and replenish ATP, which is energetically favored over expensive *de novo* synthesis. The involvement of the PPP was evidenced also by the increased abundance of riboflavin and D-erythrose 4-phosphate, which are intermediates in the PPP and precursors for the synthesis of the aromatic amino acids [111]. This, again, supports the notion of a metabolic steady-state adaptation under CHS, rerouting from glycolysis to the PPP as a metabolic transition to counteract heat stress [112–114]. Similarly, riboflavin, or vitamin B2, has been shown to play a crucial role in boosting the antioxidant and immune systems [115,116] under stress conditions. It is also possible that riboflavin could be involved in cellular oxidation and mitochondrial energy production via ETC [117] to sustain membrane stability and adequate energy-related cellular functions under CHS; however, further studies associated with the riboflavin/FAD cycle are warranted.

Partial least squares-discriminant analysis of the duodenal DA metabolites revealed a distinct separation between the HS and TN groups, indicating potential biomarkers and unique features predictive of HS. To gain further insights and identify biologically related molecule networks, we next mapped these DA metabolites to the IPA knowledge-base and analyzed the most enriched biological functions. As expected and in accordance with previous studies, both AHS and CHS affected purine nucleotide metabolism [118], urate biosynthesis/inosine 5'-phosphate degradation [119], and ascorbate recycling [120]. Interestingly, the adenosine nucleotide and dopamine degradation pathways were enriched in AHS; however, biosynthesis of UDP-D-xylose and UDP-D-glucuronate and pyrimidine salvage pathways were triggered in CHS. These changes are in consonance with previous studies [121–125]. Adenosine degradation could result in AMP or urea (via inosine) production, both of which were reported to be increased under acute heat stress conditions [126,127]. AMP increase is an indicator of ATP depletion, and urea increase has been reported as a metabolic strategy to compensate for reduced nutrient intake and increased energy expenditure under short-term heat stress exposure [126]. Dopamine has been reported to be produced by gastrointestinal tract by enteric neurons and intestinal epithelial cells in humans [128], and the dopaminergic system has been shown to be involved in stress response in many species, including avian species [122,129]. As described in previous paragraphs, IPA enrichment of the UDP-D-xylose and UDP-D-glucuronate biosynthesis and pyrimidine salvage pathways indicated a metabolic shift during CHS from glycolysis to PPP and sugar nucleotide oxidation pathways. In addition, although there is a paucity of literature in animals, UDP-D-glucuronate has been found to play a major role in drug metabolism and detoxification as well as neuroprotective function through dopamine and neurotransmitter glucuronidation [130]. In plants, however, UDP-xylose and UDP-D-glucuronate have been well established as key metabolites for stress tolerance [131–133].

The top-scoring diseases and disorders enriched by IPA from the DA metabolites were organismal and GI injury for both AHS and CHS; cancer and hematological, neurobiological, and psychological disorders in CHS; and ophthalmic, cardiovascular, developmental, and hereditary disorders in AHS. This is not surprising, as most of these disorders are associated with oxidative stress and mitochondrial dysfunction [134–138]. Of particular interest, heat stress has been reported to induce intestinal injury through the lysosome- and mitochondria-dependent pathway [139], and the identified DA metabolites in the present study could be a new vista opening for mechanistic and functional studies of the interaction of these metabolites and gut integrity under heat stress conditions. Similarly, the DA metabolites were mapped by IPA to several top molecular and cellular functions with protein synthesis, cell death and survival, and free radical scavenging enriched in CHS, while small molecule biochemistry, nucleic acid and carbohydrate metabolisms, DNA damage, and energy production were specific to AHS. This is also in agreement with previous mammalian studies [140–146] and suggests that the metabolic reprogramming and the duodenal metabolomic response pattern to environmental HS are duration-dependent. It seems that HS triggers different cellular mechanisms from favoring stress-related metabolites for averting DNA damage to adaptation/acclimatization-associated metabolites for survival.

The IPA regulatory networks identified several upstream regulators and downstream mediators. Although IPA predicted an activation of *CA9* in CHS (z score of 2) and *HDAC11* in PF (z score of 2), real-time quantitative PCR showed that these genes were downregulated by both heat stress conditions, indicating a potential feedback loop. Both *CA9* and *HDAC11* have been shown to be involved in mitochondrial function and many anomalies including stress, hypoxia and alkalosis [147–150], all of which are associated with heat stress [31,151,152]. In support of IPA-network prediction, molecular analyses demonstrated that CHS affected the duodenal expression of *MAPK1*, *MAPK14*, *MAPK9*, *SOD1*, and *SOD2* genes. The roles of these pathways in oxidative stress and cellular signaling are well established. SODs are key antioxidant enzymes that catalyze the dismutation of superoxide radicals to hydrogen peroxide [153]. Their reduced expression in our study is puzzling because most of the curated literature reported an increased activity under short-term heat stress exposure [154,155]. Although speculative, it is possible that the reduced SOD expression is associated with an exhaustion of the antioxidant defense system [156–158] in stabilizing duodenum integrity and adapting to CHS. Similarly, it has been shown that cells respond to high temperature by activating MAPKs [159–161], which are known as key mediators of stress responses. Their reduced expression in our experimental conditions suggests that the birds were adapted to CHS [162–165]. Furthermore, the CHS-induced metabolites have been shown to affect MAPKs. Indeed, salicylate, NAD^+ , NADH , and nucleosides were found to regulate the expression of MAPKs [166–169], which in turn have been reported to regulate metabolic reprogramming [170]. It is, however, worth mentioning that we measured only mRNA levels, and it is conceivable that the protein levels, enzymatic activity, and/or posttranslational modifications (phosphorylation) of these SODs were affected differently.

In conclusion, this study is the first to use a high-throughput mass spectrometric metabolomics approach to probe the heat stress-induced duodenal metabolic changes in broilers. Our results demonstrated that, independently of feed intake depression, HS induced significant changes in metabolic pathways in a duration-dependent manner and identified potential duodenal markers for HS. Although this data-driven approach was not designed to provide mechanistic and functional evidence, the IPA and molecular analyses provided additional understanding of HS responses in broiler duodenum and opened a new vista for future investigations.

Supplementary Materials: The following supporting information can be downloaded at: <https://www.mdpi.com/article/10.3390/ani12111337/s1>, Table S1. Duodenal metabolite profile in heat stressed broilers.

Author Contributions: S.D. designed the experiment and purchased the reagents. E.S.G. and S.D. conducted the trial and processed the animals at the end of the trial. S.D., A.R. and C.W.M. measured gene and protein expression. C.J.C., H.F.C. and S.R.C. performed the metabolomics analysis. G.B. determined the Venn diagrams using the R program. J.S.D. and S.D. wrote the manuscript with input from all authors. All authors have read and agreed to the published version of the manuscript.

Funding: This study was supported by a grant from Adisseo-Animal Nutrition (Award # FY2020 to Sami Dridi). Adisseo had no role in conducting the research, generating the data, interpreting the results or writing the manuscript.

Institutional Review Board Statement: All animal experiments were approved by the University of Arkansas Institutional Animal Care and Use Committee (IACUC # 21050) and were in accordance with the recommendations in *NIH's Guide for the Care and Use of Laboratory Animals*.

Informed Consent Statement: Not applicable.

Data Availability Statement: Original datasets from all studied groups have been submitted to EMBL-EBI MetaboLights database, DOI: 10.1093/nar/gkz1019, PMID:31691833) with the identifier MTBLS4513 (<https://www.ebi.ac.uk/metabolights/MTBLS4513>).

Acknowledgments: The authors would like to thank Sara Orlowski, Nima Emami, Garrett Mullenix, and the farm and processing plant crew for their technical assistance.

Conflicts of Interest: The authors declare that the research was conducted in the absence of any commercial or financial relationships that could be construed as a potential conflict of interest.

References

1. United States Department of Agriculture, Foreign Agricultural Service. *Livestock and Poultry: World Markets and Trade*; United States Department of Agriculture, Foreign Agricultural Service: Washington, DC, USA, 2022; p. 16.
2. Lara, L.J.; Rostagno, M.H. Impact of Heat Stress on Poultry Production. *Animals* **2013**, *3*, 356–369. [[CrossRef](#)] [[PubMed](#)]
3. Nawaz, A.H.; Amoah, K.; Leng, Q.Y.; Zheng, J.H.; Zhang, W.L.; Zhang, L. Poultry Response to Heat Stress: Its Physiological, Metabolic, and Genetic Implications on Meat Production and Quality Including Strategies to Improve Broiler Production in a Warming World. *Front. Vet. Sci.* **2021**, *8*, 699081. [[CrossRef](#)] [[PubMed](#)]
4. Alley, R.B.; Clark, P.U.; Huybrechts, P.; Joughin, I. Ice-sheet and sea-level changes. *Science* **2005**, *310*, 456–460. [[CrossRef](#)] [[PubMed](#)]
5. Karn, M.; Sharma, M. Climate change, natural calamities and the triple burden of disease. *Nat. Clim. Chang.* **2021**, *11*, 796–797. [[CrossRef](#)]
6. Baker, J.S.; Havlik, P.; Beach, R.; Leclere, D.; Schmid, E.; Valin, H.; Cole, J.; Creason, J.; Ohrel, S.; McFarland, J. Evaluating the effects of climate change on US agricultural systems: Sensitivity to regional impact and trade expansion scenarios. *Environ. Res. Lett.* **2018**, *13*, 064019. [[CrossRef](#)]
7. Moore, F.C.; Baldos, U.; Hertel, T.; Diaz, D. New science of climate change impacts on agriculture implies higher social cost of carbon. *Nat. Commun.* **2017**, *8*, 1607. [[CrossRef](#)]
8. Nelson, G.C.; Valin, H.; Sands, R.D.; Havlik, P.; Ahammad, H.; Deryng, D.; Elliott, J.; Fujimori, S.; Hasegawa, T.; Heyhoe, E.; et al. Climate change effects on agriculture: Economic responses to biophysical shocks. *Proc. Natl. Acad. Sci. USA* **2014**, *111*, 3274–3279. [[CrossRef](#)]
9. Rosenzweig, C.; Elliott, J.; Deryng, D.; Ruane, A.C.; Muller, C.; Arneth, A.; Boote, K.J.; Folberth, C.; Glotter, M.; Khabarov, N.; et al. Assessing agricultural risks of climate change in the 21st century in a global gridded crop model intercomparison. *Proc. Natl. Acad. Sci. USA* **2014**, *111*, 3268–3273. [[CrossRef](#)]
10. Stevanovic, M.; Popp, A.; Lotze-Campen, H.; Dietrich, J.P.; Muller, C.; Bonsch, M.; Schmitz, C.; Bodirsky, B.L.; Humpenoder, F.; Weindl, I. The impact of high-end climate change on agricultural welfare. *Sci. Adv.* **2016**, *2*, e1501452. [[CrossRef](#)]
11. Chen, I.C.; Hill, J.K.; Ohlemuller, R.; Roy, D.B.; Thomas, C.D. Rapid range shifts of species associated with high levels of climate warming. *Science* **2011**, *333*, 1024–1026. [[CrossRef](#)]
12. Liu, L.; Ren, M.; Ren, K.; Jin, Y.; Yan, M. Heat stress impacts on broiler performance: A systematic review and meta-analysis. *Poult. Sci.* **2020**, *99*, 6205–6211. [[CrossRef](#)] [[PubMed](#)]
13. Deeb, N.; Shlosberg, A.; Cahaner, A. Genotype-by-environment interaction with broiler genotypes differing in growth rate. 4. Association between responses to heat stress and to cold-induced ascites. *Poult. Sci.* **2002**, *81*, 1454–1462. [[CrossRef](#)] [[PubMed](#)]
14. Narinc, D.; Erdogan, S.; Tahtabicen, E.; Aksoy, T. Effects of thermal manipulations during embryogenesis of broiler chickens on developmental stability, hatchability and chick quality. *Animal* **2016**, *10*, 1328–1335. [[CrossRef](#)] [[PubMed](#)]

15. Emami, N.K.; Greene, E.S.; Kogut, M.H.; Dridi, S. Heat Stress and Feed Restriction Distinctly Affect Performance, Carcass and Meat Yield, Intestinal Integrity, and Inflammatory (Chemo)Cytokines in Broiler Chickens. *Front. Physiol.* **2021**, *12*, 707757. [[CrossRef](#)]
16. Orłowski, S.K.; Cauble, R.; Tabler, T.; Hiltz, J.Z.; Greene, E.S.; Anthony, N.B.; Dridi, S. Processing evaluation of random bred broiler populations and a common ancestor at 55 days under chronic heat stress conditions. *Poult. Sci.* **2020**, *99*, 3491–3500. [[CrossRef](#)] [[PubMed](#)]
17. Greene, E.S.; Cauble, R.; Kadhim, H.; de Almeida Mallmann, B.; Gu, I.; Lee, S.O.; Orłowski, S.; Dridi, S. Protective effects of the phytogetic feed additive "comfort" on growth performance via modulation of hypothalamic feeding- and drinking-related neuropeptides in cyclic heat-stressed broilers. *Domest. Anim. Endocrinol.* **2021**, *74*, 106487. [[CrossRef](#)]
18. Baxter, M.F.A.; Greene, E.S.; Kidd, M.T.; Tellez-Isaias, G.; Orłowski, S.; Dridi, S. Water amino acid-chelated trace mineral supplementation decreases circulating and intestinal HSP70 and proinflammatory cytokine gene expression in heat-stressed broiler chickens. *J. Anim. Sci.* **2020**, *98*, skaa049. [[CrossRef](#)]
19. Cahaner, A.; Leenstra, F. Effects of high temperature on growth and efficiency of male and female broilers from lines selected for high weight gain, favorable feed conversion, and high or low fat content. *Poult. Sci.* **1992**, *71*, 1237–1250. [[CrossRef](#)]
20. Leenstra, F.; Cahaner, A. Effects of low, normal, and high temperatures on slaughter yield of broilers from lines selected for high weight gain, favorable feed conversion, and high or low fat content. *Poult. Sci.* **1992**, *71*, 1994–2006. [[CrossRef](#)]
21. Dale, N.M.; Fuller, H.L. Effect of diet composition on feed intake and growth of chicks under heat stress. II. Constant vs. cycling temperatures. *Poult. Sci.* **1980**, *59*, 1434–1441. [[CrossRef](#)]
22. Quinteiro-Filho, W.M.; Ribeiro, A.; Ferraz-de-Paula, V.; Pinheiro, M.L.; Sakai, M.; Sa, L.R.; Ferreira, A.J.; Palermo-Neto, J. Heat stress impairs performance parameters, induces intestinal injury, and decreases macrophage activity in broiler chickens. *Poult. Sci.* **2010**, *89*, 1905–1914. [[CrossRef](#)] [[PubMed](#)]
23. Mitchell, M.A.; Carlisle, A.J. The effects of chronic exposure to elevated environmental temperature on intestinal morphology and nutrient absorption in the domestic fowl (*Gallus domesticus*). *Comp. Biochem. Physiol. Part A Comp. Physiol.* **1992**, *101*, 137–142. [[CrossRef](#)]
24. Jones, M.P.; Dilley, J.B.; Drossman, D.; Crowell, M.D. Brain-gut connections in functional GI disorders: Anatomic and physiologic relationships. *Neurogastroenterol. Motil.* **2006**, *18*, 91–103. [[CrossRef](#)] [[PubMed](#)]
25. Brzozowski, B.; Mazur-Bialy, A.; Pajdo, R.; Kwiecien, S.; Bilski, J.; Zwolinska-Wcislo, M.; Mach, T.; Brzozowski, T. Mechanisms by which Stress Affects the Experimental and Clinical Inflammatory Bowel Disease (IBD): Role of Brain-Gut Axis. *Curr. Neuropharmacol.* **2016**, *14*, 892–900. [[CrossRef](#)] [[PubMed](#)]
26. Breit, S.; Kupferberg, A.; Rogler, G.; Hasler, G. Vagus Nerve as Modulator of the Brain-Gut Axis in Psychiatric and Inflammatory Disorders. *Front. Psychiatry* **2018**, *9*, 44. [[CrossRef](#)] [[PubMed](#)]
27. Mukhtar, K.; Nawaz, H.; Abid, S. Functional gastrointestinal disorders and gut-brain axis: What does the future hold? *World J. Gastroenterol.* **2019**, *25*, 552–566. [[CrossRef](#)]
28. Lambert, G.P. Stress-induced gastrointestinal barrier dysfunction and its inflammatory effects. *J. Anim. Sci.* **2009**, *87*, E101–E108. [[CrossRef](#)]
29. Tur, J.A.; Rial, R.V. The effect of temperature and relative humidity on the gastrointestinal motility of young broilers. *Comp. Biochem. Physiol. Part. A Physiol.* **1985**, *80*, 481–486. [[CrossRef](#)]
30. Hai, L.; Rong, D.; Zhang, Z.Y. The effect of thermal environment on the digestion of broilers. *Anim. Physiol. Anim. Nutr.* **2000**, *83*, 57–64. [[CrossRef](#)]
31. Hall, D.M.; Baumgardner, K.R.; Oberley, T.D.; Gisolfi, C.V. Splanchnic tissues undergo hypoxic stress during whole body hyperthermia. *Am. J. Physiol.* **1999**, *276*, G1195–G1203. [[CrossRef](#)]
32. Wolfenson, D. Blood flow through arteriovenous anastomoses and its thermal function in the laying hen. *J. Physiol.* **1983**, *334*, 395–407. [[CrossRef](#)] [[PubMed](#)]
33. Ophir, E.; Arieli, Y.; Marder, J.; Horowitz, M. Cutaneous blood flow in the pigeon *Columba livia*: Its possible relevance to cutaneous water evaporation. *J. Exp. Biol.* **2002**, *205*, 2627–2636. [[CrossRef](#)] [[PubMed](#)]
34. Wolf, B.O.; Walsberg, G.E. The role of the plumage in heat transfer processes of birds. *Am. Zool.* **2000**, *40*, 575–584. [[CrossRef](#)]
35. Varasteh, S.; Braber, S.; Akbari, P.; Garssen, J.; Fink-Gremmels, J. Differences in Susceptibility to Heat Stress along the Chicken Intestine and the Protective Effects of Galacto-Oligosaccharides. *PLoS ONE* **2015**, *10*, e0138975. [[CrossRef](#)]
36. Rostagno, M.H. Effects of heat stress on the gut health of poultry. *J. Anim. Sci.* **2020**, *98*, skaa090. [[CrossRef](#)]
37. Alhenaky, A.; Abdelqader, A.; Abuajamieh, M.; Al-Fataftah, A.R. The effect of heat stress on intestinal integrity and Salmonella invasion in broiler birds. *J. Therm. Biol.* **2017**, *70*, 9–14. [[CrossRef](#)]
38. Quinteiro-Filho, W.M.; Gomes, A.V.; Pinheiro, M.L.; Ribeiro, A.; Ferraz-de-Paula, V.; Astolfi-Ferreira, C.S.; Ferreira, A.J.; Palermo-Neto, J. Heat stress impairs performance and induces intestinal inflammation in broiler chickens infected with Salmonella Enteritidis. *Avian Pathol.* **2012**, *41*, 421–427. [[CrossRef](#)]
39. Tsiouris, V.; Georgopoulou, I.; Batzios, C.; Pappaioannou, N.; Ducatelle, R.; Fortomaris, P. Heat stress as a predisposing factor for necrotic enteritis in broiler chicks. *Avian Pathol.* **2018**, *47*, 616–624. [[CrossRef](#)]
40. Kaldhusdal, M.; Benestad, S.L.; Lovland, A. Epidemiologic aspects of necrotic enteritis in broiler chickens—Disease occurrence and production performance. *Avian Pathol.* **2016**, *45*, 271–274. [[CrossRef](#)]

41. Kadykalo, S.; Roberts, T.; Thompson, M.; Wilson, J.; Lang, M.; Espeisse, O. The value of anticoccidials for sustainable global poultry production. *Int. J. Antimicrob. Agents* **2018**, *51*, 304–310. [[CrossRef](#)]
42. Skinner, J.T.; Bauer, S.; Young, V.; Pauling, G.; Wilson, J. An economic analysis of the impact of subclinical (mild) necrotic enteritis in broiler chickens. *Avian Dis.* **2010**, *54*, 1237–1240. [[CrossRef](#)] [[PubMed](#)]
43. Mora, C.; Frazier, A.G.; Longman, R.J.; Dacks, R.S.; Walton, M.M.; Tong, E.J.; Sanchez, J.J.; Kaiser, L.R.; Stender, Y.O.; Anderson, J.M.; et al. The projected timing of climate departure from recent variability. *Nature* **2013**, *502*, 183–187. [[CrossRef](#)] [[PubMed](#)]
44. Moss, R.H.; Edmonds, J.A.; Hibbard, K.A.; Manning, M.R.; Rose, S.K.; van Vuuren, D.P.; Carter, T.R.; Emori, S.; Kainuma, M.; Kram, T.; et al. The next generation of scenarios for climate change research and assessment. *Nature* **2010**, *463*, 747–756. [[CrossRef](#)] [[PubMed](#)]
45. Trisos, C.H.; Merow, C.; Pigot, A.L. The projected timing of abrupt ecological disruption from climate change. *Nature* **2020**, *580*, 496–501. [[CrossRef](#)] [[PubMed](#)]
46. Tabler, T.W.; Greene, E.S.; Orłowski, S.K.; Hiltz, J.Z.; Anthony, N.B.; Dridi, S. Intestinal Barrier Integrity in Heat-Stressed Modern Broilers and Their Ancestor Wild Jungle Fowl. *Front. Vet. Sci.* **2020**, *7*, 249. [[CrossRef](#)] [[PubMed](#)]
47. Ruff, J.; Barros, T.L.; Tellez, G., Jr.; Blankenship, J.; Lester, H.; Graham, B.D.; Selby, C.A.M.; Vuong, C.N.; Dridi, S.; Greene, E.S.; et al. Research Note: Evaluation of a heat stress model to induce gastrointestinal leakage in broiler chickens. *Poult. Sci.* **2020**, *99*, 1687–1692. [[CrossRef](#)]
48. Greene, E.; Cauble, R.; Dhamad, A.E.; Kidd, M.T.; Kong, B.; Howard, S.M.; Castro, H.F.; Campagna, S.R.; Bedford, M.; Dridi, S. Muscle Metabolome Profiles in Woody Breast-(un)Affected Broilers: Effects of Quantum Blue Phytase-Enriched Diet. *Front. Vet. Sci.* **2020**, *7*, 458. [[CrossRef](#)]
49. Clemmons, B.A.; Martino, C.; Powers, J.B.; Campagna, S.R.; Voy, B.H.; Donohoe, D.R.; Gaffney, J.; Embree, M.M.; Myer, P.R. Rumen Bacteria and Serum Metabolites Predictive of Feed Efficiency Phenotypes in Beef Cattle. *Sci. Rep.* **2019**, *9*, 19265. [[CrossRef](#)]
50. Lu, W.; Clasquin, M.F.; Melamud, E.; Amador-Nogues, D.; Caudy, A.A.; Rabinowitz, J.D. Metabolomic analysis via reversed-phase ion-pairing liquid chromatography coupled to a stand alone orbitrap mass spectrometer. *Anal. Chem.* **2010**, *82*, 3212–3221. [[CrossRef](#)]
51. Kessner, D.; Chambers, M.; Burke, R.; Agus, D.; Mallick, P. ProteoWizard: Open source software for rapid proteomics tools development. *Bioinformatics* **2008**, *24*, 2534–2536. [[CrossRef](#)]
52. Chambers, M.C.; Maclean, B.; Burke, R.; Amodei, D.; Ruderman, D.L.; Neumann, S.; Gatto, L.; Fischer, B.; Pratt, B.; Egertson, J.; et al. A cross-platform toolkit for mass spectrometry and proteomics. *Nat. Biotechnol.* **2012**, *30*, 918–920. [[CrossRef](#)] [[PubMed](#)]
53. Clasquin, M.F.; Melamud, E.; Rabinowitz, J.D. LC-MS data processing with MAVEN: A metabolomic analysis and visualization engine. *Curr. Protoc. Bioinform.* **2012**, *37*, 14.11.1–14.11.23. [[CrossRef](#)]
54. Bazurto, J.V.; Dearth, S.P.; Tague, E.D.; Campagna, S.R.; Downs, D.M. Untargeted metabolomics confirms and extends the understanding of the impact of aminoimidazole carboxamide ribotide (AICAR) in the metabolic network of *Salmonella enterica*. *Microb. Cell* **2017**, *5*, 74–87. [[CrossRef](#)] [[PubMed](#)]
55. Wishart, D.S.; Feunang, Y.D.; Marcu, A.; Guo, A.C.; Liang, K.; Vazquez-Fresno, R.; Sajed, T.; Johnson, D.; Li, C.; Karu, N.; et al. HMDB 4.0: The human metabolome database for 2018. *Nucleic Acids Res.* **2018**, *46*, D608–D617. [[CrossRef](#)] [[PubMed](#)]
56. Kanehisa, M.; Furumichi, M.; Tanabe, M.; Sato, Y.; Morishima, K. KEGG: New perspectives on genomes, pathways, diseases and drugs. *Nucleic Acids Res.* **2017**, *45*, D353–D361. [[CrossRef](#)] [[PubMed](#)]
57. Hastings, J.; Owen, G.; Dekker, A.; Ennis, M.; Kale, N.; Muthukrishnan, V.; Turner, S.; Swainston, N.; Mendes, P.; Steinbeck, C. ChEBI in 2016: Improved services and an expanding collection of metabolites. *Nucleic Acids Res.* **2016**, *44*, D1214–D1219. [[CrossRef](#)]
58. Rajaei-Sharifabadi, H.; Ellestad, L.; Porter, T.; Donoghue, A.; Bottje, W.G.; Dridi, S. Noni (*Morinda citrifolia*) Modulates the Hypothalamic Expression of Stress- and Metabolic-Related Genes in Broilers Exposed to Acute Heat Stress. *Front. Genet.* **2017**, *8*, 192. [[CrossRef](#)]
59. Piekarski, A.; Nagarajan, G.; Ishola, P.; Flees, J.; Greene, E.S.; Kuenzel, W.J.; Ohkubo, T.; Maier, H.; Bottje, W.G.; Cline, M.A.; et al. AMP-Activated Protein Kinase Mediates the Effect of Leptin on Avian Autophagy in a Tissue-Specific Manner. *Front. Physiol.* **2018**, *9*, 541. [[CrossRef](#)]
60. Dhamad, A.E.; Greene, E.; Sales, M.; Nguyen, P.; Beer, L.; Liyanage, R.; Dridi, S. 75-kDa glucose-regulated protein (GRP75) is a novel molecular signature for heat stress response in avian species. *Am. J. Physiol. Cell Physiol.* **2020**, *318*, C289–C303. [[CrossRef](#)]
61. Ferver, A.; Dridi, S. Regulation of avian uncoupling protein (av-UCP) expression by cytokines and hormonal signals in quail myoblast cells. *Comp. Biochem. Physiol. A Mol. Integr. Physiol.* **2020**, *248*, 110747. [[CrossRef](#)]
62. Schmittgen, T.D.; Livak, K.J. Analyzing real-time PCR data by the comparative C(T) method. *Nat. Protoc.* **2008**, *3*, 1101–1108. [[CrossRef](#)] [[PubMed](#)]
63. Dridi, S.; Hirano, Y.; Tarallo, V.; Kim, Y.; Fowler, B.J.; Ambati, B.K.; Bogdanovich, S.; Chiodo, V.A.; Hauswirth, W.W.; Kugel, J.F.; et al. ERK1/2 activation is a therapeutic target in age-related macular degeneration. *Proc. Natl. Acad. Sci. USA* **2012**, *109*, 13781–13786. [[CrossRef](#)] [[PubMed](#)]
64. de Hoon, M.J.; Imoto, S.; Nolan, J.; Miyano, S. Open source clustering software. *Bioinformatics* **2004**, *20*, 1453–1454. [[CrossRef](#)] [[PubMed](#)]
65. Saldanha, A.J. Java Treeview—extensible visualization of microarray data. *Bioinformatics* **2004**, *20*, 3246–3248. [[CrossRef](#)]

66. Pang, Z.; Chong, J.; Zhou, G.; de Lima Morais, D.A.; Chang, L.; Barrette, M.; Gauthier, C.; Jacques, P.E.; Li, S.; Xia, J. MetaboAnalyst 5.0: Narrowing the gap between raw spectra and functional insights. *Nucleic Acids Res.* **2021**, *49*, W388–W396. [[CrossRef](#)]
67. St-Pierre, N.R.; Cobanov, B.; Schnitkey, G. Economic Losses from Heat Stress by US Livestock Industries. *J. Dairy Sci.* **2003**, *86*, E52–E77. [[CrossRef](#)]
68. Zaboli, G.; Huang, X.; Feng, X.; Ahn, D.U. How can heat stress affect chicken meat quality?—a review. *Poult. Sci.* **2019**, *98*, 1551–1556. [[CrossRef](#)]
69. Hirakawa, R.; Nurjanah, S.; Furukawa, K.; Murai, A.; Kikusato, M.; Nochi, T.; Toyomizu, M. Heat Stress Causes Immune Abnormalities via Massive Damage to Effect Proliferation and Differentiation of Lymphocytes in Broiler Chickens. *Front. Vet. Sci.* **2020**, *7*, 46. [[CrossRef](#)]
70. Piestun, Y.; Patael, T.; Yahav, S.; Velleman, S.G.; Halevy, O. Early posthatch thermal stress affects breast muscle development and satellite cell growth and characteristics in broilers. *Poult. Sci.* **2017**, *96*, 2877–2888. [[CrossRef](#)]
71. Tang, S.; Zhou, S.; Yin, B.; Xu, J.; Di, L.; Zhang, J.; Bao, E. Heat stress-induced renal damage in poultry and the protective effects of HSP60 and HSP47. *Cell Stress Chaperones* **2018**, *23*, 1033–1040. [[CrossRef](#)]
72. Song, J.; Xiao, K.; Ke, Y.L.; Jiao, L.F.; Hu, C.H.; Diao, Q.Y.; Shi, B.; Zou, X.T. Effect of a probiotic mixture on intestinal microflora, morphology, and barrier integrity of broilers subjected to heat stress. *Poult. Sci.* **2014**, *93*, 581–588. [[CrossRef](#)] [[PubMed](#)]
73. Bujak, R.; Struck-Lewicka, W.; Markuszewski, M.J.; Kaliszán, R. Metabolomics for laboratory diagnostics. *J. Pharm. Biomed. Anal.* **2015**, *113*, 108–120. [[CrossRef](#)] [[PubMed](#)]
74. Hermes, J.D.; Tipton, P.A.; Fisher, M.A.; O’Leary, M.H.; Morrison, J.F.; Cleland, W.W. Mechanisms of enzymatic and acid-catalyzed decarboxylations of prephenate. *Biochemistry* **1984**, *23*, 6263–6275. [[CrossRef](#)] [[PubMed](#)]
75. Maeda, H.; Dudareva, N. The shikimate pathway and aromatic amino Acid biosynthesis in plants. *Annu. Rev. Plant Biol.* **2012**, *63*, 73–105. [[CrossRef](#)]
76. Manandhar, M.; Cronan, J.E. Pimelic acid, the first precursor of the *Bacillus subtilis* biotin synthesis pathway, exists as the free acid and is assembled by fatty acid synthesis. *Mol. Microbiol.* **2017**, *104*, 595–607. [[CrossRef](#)] [[PubMed](#)]
77. Tang, W.; Jiang, H.; Zheng, Q.; Chen, X.; Wang, R.; Yang, S.; Zhao, G.; Liu, J.; Norvienyeku, J.; Wang, Z. Isopropylmalate isomerase MoLeu1 orchestrates leucine biosynthesis, fungal development, and pathogenicity in *Magnaporthe oryzae*. *Appl. Microbiol. Biotechnol.* **2019**, *103*, 327–337. [[CrossRef](#)]
78. He, Y.; Chen, B.; Pang, Q.; Strul, J.M.; Chen, S. Functional specification of *Arabidopsis* isopropylmalate isomerases in glucosinolate and leucine biosynthesis. *Plant. Cell Physiol.* **2010**, *51*, 1480–1487. [[CrossRef](#)]
79. Kers, J.G.; Velkers, F.C.; Fischer, E.A.J.; Hermes, G.D.A.; Stegeman, J.A.; Smidt, H. Host and Environmental Factors Affecting the Intestinal Microbiota in Chickens. *Front. Microbiol.* **2018**, *9*, 235. [[CrossRef](#)]
80. Shi, D.; Bai, L.; Qu, Q.; Zhou, S.; Yang, M.; Guo, S.; Li, Q.; Liu, C. Impact of gut microbiota structure in heat-stressed broilers. *Poult. Sci.* **2019**, *98*, 2405–2413. [[CrossRef](#)]
81. Gallardo, M.E.; Desviat, L.R.; Rodriguez, J.M.; Esparza-Gordillo, J.; Perez-Cerda, C.; Perez, B.; Rodriguez-Pombo, P.; Criado, O.; Sanz, R.; Morton, D.H.; et al. The molecular basis of 3-methylcrotonylglycinuria, a disorder of leucine catabolism. *Am. J. Hum. Genet.* **2001**, *68*, 334–346. [[CrossRef](#)]
82. Bartlett, K.; Ng, H.; Leonard, J.V. A combined defect of three mitochondrial carboxylases presenting as biotin-responsive 3-methylcrotonyl glycinuria and 3-hydroxyisovaleric aciduria. *Clin. Chim. Acta* **1980**, *100*, 183–186. [[CrossRef](#)]
83. Liebich, H.M.; Forst, C. Hydroxycarboxylic and oxocarboxylic acids in urine: Products from branched-chain amino acid degradation and from ketogenesis. *J. Chromatogr.* **1984**, *309*, 225–242. [[CrossRef](#)]
84. Tamura, Y.; Kitaoka, Y.; Matsunaga, Y.; Hoshino, D.; Hatta, H. Daily heat stress treatment rescues denervation-activated mitochondrial clearance and atrophy in skeletal muscle. *J. Physiol.* **2015**, *593*, 2707–2720. [[CrossRef](#)] [[PubMed](#)]
85. Mujahid, A.; Akiba, Y.; Toyomizu, M. Acute heat stress induces oxidative stress and decreases adaptation in young white leghorn cockerels by downregulation of avian uncoupling protein. *Poult. Sci.* **2007**, *86*, 364–371. [[CrossRef](#)] [[PubMed](#)]
86. Zhao, H.; Jiang, Z.; Chang, X.; Xue, H.; Yahefu, W.; Zhang, X. 4-Hydroxyphenylacetic Acid Prevents Acute APAP-Induced Liver Injury by Increasing Phase II and Antioxidant Enzymes in Mice. *Front. Pharmacol.* **2018**, *9*, 653. [[CrossRef](#)]
87. Dangl, J. Innate immunity. Plants just say NO to pathogens. *Nature* **1998**, *394*, 525. [[CrossRef](#)]
88. Gamble-George, J.C.; Baldi, R.; Halladay, L.; Kocharian, A.; Hartley, N.; Silva, C.G.; Roberts, H.; Haymer, A.; Marnett, L.J.; Holmes, A.; et al. Cyclooxygenase-2 inhibition reduces stress-induced affective pathology. *Elife* **2016**, *5*, e14137. [[CrossRef](#)]
89. Guo, J.Y.; Li, C.Y.; Ruan, Y.P.; Sun, M.; Qi, X.L.; Zhao, B.S.; Luo, F. Chronic treatment with celecoxib reverses chronic unpredictable stress-induced depressive-like behavior via reducing cyclooxygenase-2 expression in rat brain. *Eur. J. Pharmacol.* **2009**, *612*, 54–60. [[CrossRef](#)]
90. Kumari, B.; Kumar, A.; Dhir, A. Protective effect of non-selective and selective CO_{x-2}-inhibitors in acute immobilization stress-induced behavioral and biochemical alterations. *Pharmacol. Rep.* **2007**, *59*, 699–707.
91. Rossi, A.; Coccia, M.; Trotta, E.; Angelini, M.; Santoro, M.G. Regulation of cyclooxygenase-2 expression by heat: A novel aspect of heat shock factor 1 function in human cells. *PLoS ONE* **2012**, *7*, e31304. [[CrossRef](#)]
92. Moon, E.J.; Sonveaux, P.; Porporato, P.E.; Danhier, P.; Gallez, B.; Batinic-Haberle, I.; Nien, Y.C.; Schroeder, T.; Dewhirst, M.W. NADPH oxidase-mediated reactive oxygen species production activates hypoxia-inducible factor-1 (HIF-1) via the ERK pathway after hyperthermia treatment. *Proc. Natl. Acad. Sci. USA* **2010**, *107*, 20477–20482. [[CrossRef](#)] [[PubMed](#)]
93. Segal, A.W.; Abo, A. The biochemical basis of the NADPH oxidase of phagocytes. *Trends Biochem. Sci.* **1993**, *18*, 43–47. [[CrossRef](#)]

94. Hirst, J. Towards the molecular mechanism of respiratory complex I. *Biochem. J.* **2009**, *425*, 327–339. [[CrossRef](#)] [[PubMed](#)]
95. Yang, C.; Luo, P.; Chen, S.J.; Deng, Z.C.; Fu, X.L.; Xu, D.N.; Tian, Y.B.; Huang, Y.M.; Liu, W.J. Resveratrol sustains intestinal barrier integrity, improves antioxidant capacity, and alleviates inflammation in the jejunum of ducks exposed to acute heat stress. *Poult. Sci.* **2021**, *100*, 101459. [[CrossRef](#)] [[PubMed](#)]
96. Azad, M.A.; Kikusato, M.; Sudo, S.; Amo, T.; Toyomizu, M. Time course of ROS production in skeletal muscle mitochondria from chronic heat-exposed broiler chicken. *Comp. Biochem. Physiol. A Mol. Integr. Physiol.* **2010**, *157*, 266–271. [[CrossRef](#)] [[PubMed](#)]
97. Mracek, T.; Drahotka, Z.; Houstek, J. The function and the role of the mitochondrial glycerol-3-phosphate dehydrogenase in mammalian tissues. *Biochim. Biophys. Acta* **2013**, *1827*, 401–410. [[CrossRef](#)] [[PubMed](#)]
98. Mracek, T.; Holzerova, E.; Drahotka, Z.; Kovarova, N.; Vrbacky, M.; Jesina, P.; Houstek, J. ROS generation and multiple forms of mammalian mitochondrial glycerol-3-phosphate dehydrogenase. *Biochim. Biophys. Acta* **2014**, *1837*, 98–111. [[CrossRef](#)]
99. McCormack, J.G.; Denton, R.M. The role of Ca²⁺ in the regulation of intramitochondrial energy production in heart. *Biomed Biochim. Acta* **1987**, *46*, S487–S492.
100. Furukawa, A.; Tada-Oikawa, S.; Kawanishi, S.; Oikawa, S. H₂O₂ accelerates cellular senescence by accumulation of acetylated p53 via decrease in the function of SIRT1 by NAD⁺ depletion. *Cell. Physiol. Biochem.* **2007**, *20*, 45–54. [[CrossRef](#)]
101. Ying, W. NAD⁺ and NADH in brain functions, brain diseases and brain aging. *Front. Biosci.* **2007**, *12*, 1863–1888. [[CrossRef](#)]
102. Ying, W.; Wei, G.; Wang, D.; Wang, Q.; Tang, X.; Shi, J.; Zhang, P.; Lu, H. Intranasal administration with NAD⁺ profoundly decreases brain injury in a rat model of transient focal ischemia. *Front. Biosci.* **2007**, *12*, 2728–2734. [[CrossRef](#)] [[PubMed](#)]
103. Houtkooper, R.H.; Canto, C.; Wanders, R.J.; Auwerx, J. The secret life of NAD⁺: An old metabolite controlling new metabolic signaling pathways. *Endocr. Rev.* **2010**, *31*, 194–223. [[CrossRef](#)] [[PubMed](#)]
104. Arnaud, C.; Joyeux-Faure, M.; Godin-Ribuot, D.; Ribuot, C. CO_{x-2}: An in vivo evidence of its participation in heat stress-induced myocardial preconditioning. *Cardiovasc. Res.* **2003**, *58*, 582–588. [[CrossRef](#)]
105. Arnaud, C.; Godin-Ribuot, D.; Bottari, S.; Peinnequin, A.; Joyeux, M.; Demenge, P.; Ribuot, C. iNOS is a mediator of the heat stress-induced preconditioning against myocardial infarction in vivo in the rat. *Cardiovasc. Res.* **2003**, *58*, 118–125. [[CrossRef](#)]
106. Canto, C.; Menzies, K.J.; Auwerx, J. NAD(+) Metabolism and the Control of Energy Homeostasis: A Balancing Act between Mitochondria and the Nucleus. *Cell Metab.* **2015**, *22*, 31–53. [[CrossRef](#)]
107. Cerutti, R.; Pirinen, E.; Lamperti, C.; Marchet, S.; Sauve, A.A.; Li, W.; Leoni, V.; Schon, E.A.; Dantzer, F.; Auwerx, J.; et al. NAD(+)-dependent activation of Sirt1 corrects the phenotype in a mouse model of mitochondrial disease. *Cell Metab.* **2014**, *19*, 1042–1049. [[CrossRef](#)]
108. Mouchiroud, L.; Houtkooper, R.H.; Moullan, N.; Katsyuba, E.; Ryu, D.; Canto, C.; Mottis, A.; Jo, Y.S.; Viswanathan, M.; Schoonjans, K.; et al. The NAD(+)/Sirtuin Pathway Modulates Longevity through Activation of Mitochondrial UPR and FOXO Signaling. *Cell* **2013**, *154*, 430–441. [[CrossRef](#)]
109. Koch, F.; Albrecht, D.; Gors, S.; Kuhla, B. Jejunal mucosa proteomics unravel metabolic adaptive processes to mild chronic heat stress in dairy cows. *Sci. Rep.* **2021**, *11*, 12484. [[CrossRef](#)]
110. Milanese, C.; Bombardieri, C.R.; Sepe, S.; Barnhoorn, S.; Payan-Gomez, C.; Caruso, D.; Audano, M.; Pedretti, S.; Vermeij, W.P.; Brandt, R.M.C.; et al. DNA damage and transcription stress cause ATP-mediated redesign of metabolism and potentiation of anti-oxidant buffering. *Nat. Commun.* **2019**, *10*, 4887. [[CrossRef](#)]
111. Horecker, B.L. The pentose phosphate pathway. *J. Biol. Chem.* **2002**, *277*, 47965–47971. [[CrossRef](#)]
112. Ralser, M.; Wamelink, M.M.; Kowald, A.; Gerisch, B.; Heeren, G.; Struys, E.A.; Klipp, E.; Jakobs, C.; Breitenbach, M.; Lehrach, H.; et al. Dynamic rerouting of the carbohydrate flux is key to counteracting oxidative stress. *J. Biol.* **2007**, *6*, 10. [[CrossRef](#)] [[PubMed](#)]
113. Ralser, M.; Wamelink, M.M.; Latkolik, S.; Jansen, E.E.; Lehrach, H.; Jakobs, C. Metabolic reconfiguration precedes transcriptional regulation in the antioxidant response. *Nat. Biotechnol.* **2009**, *27*, 604–605. [[CrossRef](#)] [[PubMed](#)]
114. Cosentino, C.; Grieco, D.; Costanzo, V. ATM activates the pentose phosphate pathway promoting anti-oxidant defence and DNA repair. *EMBO J.* **2011**, *30*, 546–555. [[CrossRef](#)] [[PubMed](#)]
115. Alam, M.M.; Iqbal, S.; Naseem, I. Ameliorative effect of riboflavin on hyperglycemia, oxidative stress and DNA damage in type-2 diabetic mice: Mechanistic and therapeutic strategies. *Arch. Biochem. Biophys.* **2015**, *584*, 10–19. [[CrossRef](#)]
116. Suwannasom, N.; Kao, I.; Pruss, A.; Georgieva, R.; Baumler, H. Riboflavin: The Health Benefits of a Forgotten Natural Vitamin. *Int. J. Mol. Sci.* **2020**, *21*, 950. [[CrossRef](#)]
117. Powers, H.J. Riboflavin (vitamin B-2) and health. *Am. J. Clin. Nutr.* **2003**, *77*, 1352–1360. [[CrossRef](#)]
118. Ippolito, D.L.; Lewis, J.A.; Yu, C.; Leon, L.R.; Stallings, J.D. Alteration in circulating metabolites during and after heat stress in the conscious rat: Potential biomarkers of exposure and organ-specific injury. *BMC Physiol.* **2014**, *14*, 14. [[CrossRef](#)]
119. Knochel, J.P.; Dotin, L.N.; Hamburger, R.J. Heat stress, exercise, and muscle injury: Effects on urate metabolism and renal function. *Ann. Intern. Med.* **1974**, *81*, 321–328. [[CrossRef](#)]
120. Massot, C.; Bancel, D.; Lopez Lauri, F.; Truffault, V.; Baldet, P.; Stevens, R.; Gautier, H. High temperature inhibits ascorbate recycling and light stimulation of the ascorbate pool in tomato despite increased expression of biosynthesis genes. *PLoS ONE* **2013**, *8*, e84474. [[CrossRef](#)]
121. Fredholm, B.B. Adenosine, an endogenous distress signal, modulates tissue damage and repair. *Cell Death Differ.* **2007**, *14*, 1315–1323. [[CrossRef](#)]

122. Calefi, A.S.; Fonseca, J.; Nunes, C.A.Q.; Lima, A.P.N.; Quinteiro-Filho, W.M.; Florio, J.C.; Zager, A.; Ferreira, A.J.P.; Palermo-Neto, J. Heat Stress Modulates Brain Monoamines and Their Metabolites Production in Broiler Chickens Co-Infected with *Clostridium perfringens* Type A and *Eimeria* spp. *Vet. Sci.* **2019**, *6*, 4. [[CrossRef](#)] [[PubMed](#)]
123. Dunn, A.J.; File, S.E. Cold restraint alters dopamine metabolism in frontal cortex, nucleus accumbens and neostriatum. *Physiol. Behav.* **1983**, *31*, 511–513. [[CrossRef](#)]
124. Gradinaru, D.; Minn, A.L.; Artur, Y.; Minn, A.; Heydel, J.M. Effect of oxidative stress on UDP-glucuronosyltransferases in rat astrocytes. *Toxicol. Lett.* **2012**, *213*, 316–324. [[CrossRef](#)]
125. Livernois, A.M.; Mallard, B.A.; Cartwright, S.L.; Canovas, A. Heat stress and immune response phenotype affect DNA methylation in blood mononuclear cells from Holstein dairy cows. *Sci. Rep.* **2021**, *11*, 11371. [[CrossRef](#)] [[PubMed](#)]
126. Garner, J.B.; Williams, S.R.O.; Wales, W.J.; Marett, L.C.; DiGiacomo, K.; Leury, B.J.; Hayes, B.J. Responses of dairy cows to short-term heat stress in controlled-climate chambers. *Anim. Prod. Sci.* **2017**, *57*, 1233–1241. [[CrossRef](#)]
127. Belhadj Slimen, I.; Najar, T.; Ghram, A.; Abdrabba, M. Heat stress effects on livestock: Molecular, cellular and metabolic aspects, a review. *J. Anim. Physiol. Anim. Nutr.* **2016**, *100*, 401–412. [[CrossRef](#)]
128. Eisenhofer, G.; Aneman, A.; Friberg, P.; Hooper, D.; Fandriks, L.; Lonroth, H.; Hunyady, B.; Mezey, E. Substantial production of dopamine in the human gastrointestinal tract. *J. Clin. Endocrinol. Metab.* **1997**, *82*, 3864–3871. [[CrossRef](#)]
129. Adell, A.; Garcia-Marquez, C.; Armario, A.; Gelpi, E. Chronic stress increases serotonin and noradrenaline in rat brain and sensitizes their responses to a further acute stress. *J. Neurochem.* **1988**, *50*, 1678–1681. [[CrossRef](#)]
130. Ouzzine, M.; Gulberti, S.; Ramalanjaona, N.; Magdalou, J.; Fournel-Gigleux, S. The UDP-glucuronosyltransferases of the blood-brain barrier: Their role in drug metabolism and detoxication. *Front. Cell. Neurosci.* **2014**, *8*, 349. [[CrossRef](#)]
131. Geng, G.; Lv, C.; Stevanato, P.; Li, R.; Liu, H.; Yu, L.; Wang, Y. Transcriptome Analysis of Salt-Sensitive and Tolerant Genotypes Reveals Salt-Tolerance Metabolic Pathways in Sugar Beet. *Int. J. Mol. Sci.* **2019**, *20*, 5910. [[CrossRef](#)]
132. Ahn, J.W.; Verma, R.; Kim, M.; Lee, J.Y.; Kim, Y.K.; Bang, J.W.; Reiter, W.D.; Pai, H.S. Depletion of UDP-D-apiose/UDP-D-xylose synthases results in rhamnogalacturonan-II deficiency, cell wall thickening, and cell death in higher plants. *J. Biol. Chem.* **2006**, *281*, 13708–13716. [[CrossRef](#)] [[PubMed](#)]
133. Le Gall, H.; Philippe, F.; Domon, J.M.; Gillet, F.; Pelloux, J.; Rayon, C. Cell Wall Metabolism in Response to Abiotic Stress. *Plants* **2015**, *4*, 112–166. [[CrossRef](#)] [[PubMed](#)]
134. Bouchama, A.; Aziz, M.A.; Mahri, S.A.; Gabere, M.N.; Dlamy, M.A.; Mohammad, S.; Abbad, M.A.; Hussein, M. A Model of Exposure to Extreme Environmental Heat Uncovers the Human Transcriptome to Heat Stress. *Sci. Rep.* **2017**, *7*, 9429. [[CrossRef](#)] [[PubMed](#)]
135. Dai, S.; Mo, Y.; Wang, Y.; Xiang, B.; Liao, Q.; Zhou, M.; Li, X.; Li, Y.; Xiong, W.; Li, G.; et al. Chronic Stress Promotes Cancer Development. *Front. Oncol.* **2020**, *10*, 1492. [[CrossRef](#)]
136. El-Boshy, M.E.; Refaat, B.; Qasem, A.H.; Khan, A.; Ghaith, M.; Almasmoum, H.; Mahbub, A.; Almaini, R.A. The remedial effect of *Thymus vulgaris* extract against lead toxicity-induced oxidative stress, hepatorenal damage, immunosuppression, and hematological disorders in rats. *Environ. Sci. Pollut. Res. Int.* **2019**, *26*, 22736–22746. [[CrossRef](#)]
137. Davis, M.T.; Holmes, S.E.; Pietrzak, R.H.; Esterlis, I. Neurobiology of Chronic Stress-Related Psychiatric Disorders: Evidence from Molecular Imaging Studies. *Chronic Stress* **2017**, *1*, 2470547017710916. [[CrossRef](#)]
138. Smith, K.E.; Pollak, S.D. Early life stress and development: Potential mechanisms for adverse outcomes. *J. Neurodev. Disord.* **2020**, *12*, 34. [[CrossRef](#)]
139. Yi, G.; Li, L.; Luo, M.; He, X.; Zou, Z.; Gu, Z.; Su, L. Heat stress induces intestinal injury through lysosome- and mitochondria-dependent pathway in vivo and in vitro. *Oncotarget* **2017**, *8*, 40741–40755. [[CrossRef](#)]
140. Duncan, R.F.; Hershey, J.W. Protein synthesis and protein phosphorylation during heat stress, recovery, and adaptation. *J. Cell Biol.* **1989**, *109*, 1467–1481. [[CrossRef](#)]
141. Thompson, S.M.; Callstrom, M.R.; Butters, K.A.; Knudsen, B.; Grande, J.P.; Roberts, L.R.; Woodrum, D.A. Heat stress induced cell death mechanisms in hepatocytes and hepatocellular carcinoma: In vitro and in vivo study. *Lasers Surg. Med.* **2014**, *46*, 290–301. [[CrossRef](#)]
142. Arnaud, C.; Joyeux, M.; Garrel, C.; Godin-Ribuot, D.; Demenge, P.; Ribouot, C. Free-radical production triggered by hyperthermia contributes to heat stress-induced cardioprotection in isolated rat hearts. *Br. J. Pharmacol.* **2002**, *135*, 1776–1782. [[CrossRef](#)] [[PubMed](#)]
143. Gao, S.T.; Ma, L.; Zhou, Z.; Zhou, Z.K.; Baumgard, L.H.; Jiang, D.; Bionaz, M.; Bu, D.P. Heat stress negatively affects the transcriptome related to overall metabolism and milk protein synthesis in mammary tissue of midlactating dairy cows. *Physiol. Genom.* **2019**, *51*, 400–409. [[CrossRef](#)] [[PubMed](#)]
144. Victoria Sanz Fernandez, M.; Johnson, J.S.; Abuajamieh, M.; Stoakes, S.K.; Seibert, J.T.; Cox, L.; Kahl, S.; Elsasser, T.H.; Ross, J.W.; Isom, S.C.; et al. Effects of heat stress on carbohydrate and lipid metabolism in growing pigs. *Physiol. Rep.* **2015**, *3*, e12315. [[CrossRef](#)] [[PubMed](#)]
145. Kantidze, O.L.; Velichko, A.K.; Luzhin, A.V.; Razin, S.V. Heat Stress-Induced DNA Damage. *Acta Nat.* **2016**, *8*, 75–78. [[CrossRef](#)]
146. Febbraio, M.A. Alterations in energy metabolism during exercise and heat stress. *Sports Med.* **2001**, *31*, 47–59. [[CrossRef](#)]
147. Xu, J.; Zhu, S.; Xu, L.; Liu, X.; Ding, W.; Wang, Q.; Chen, Y.; Deng, H. CA9 Silencing Promotes Mitochondrial Biogenesis, Increases Putrescine Toxicity and Decreases Cell Motility to Suppress ccRCC Progression. *Int. J. Mol. Sci.* **2020**, *21*, 5939. [[CrossRef](#)]

148. Swietach, P.; Patiar, S.; Supuran, C.T.; Harris, A.L.; Vaughan-Jones, R.D. The role of carbonic anhydrase 9 in regulating extracellular and intracellular pH in three-dimensional tumor cell growths. *J. Biol. Chem.* **2009**, *284*, 20299–20310. [[CrossRef](#)]
149. Sun, L.; Marin de Evsikova, C.; Bian, K.; Achille, A.; Telles, E.; Pei, H.; Seto, E. Programming and Regulation of Metabolic Homeostasis by HDAC11. *EBioMedicine* **2018**, *33*, 157–168. [[CrossRef](#)]
150. Kumar, R.; Jain, V.; Kushwah, N.; Dheer, A.; Mishra, K.P.; Prasad, D.; Singh, S.B. HDAC inhibition prevents hypobaric hypoxia-induced spatial memory impairment through PI3K/Akt/GSK3 β /CREB pathway. *J. Cell. Physiol.* **2021**, *236*, 6754–6771. [[CrossRef](#)]
151. Odom, T.W.; Harrison, P.C.; Bottje, W.G. Effects of thermal-induced respiratory alkalosis on blood ionized calcium levels in the domestic hen. *Poult. Sci.* **1986**, *65*, 570–573. [[CrossRef](#)]
152. Cottrell, J.J.; Furness, J.B.; Wijesiriwardana, U.A.; Ringuet, M.; Liu, F.; DiGiacomo, K.; Leury, B.J.; Clarke, I.J.; Dunshea, F.R. The Effect of Heat Stress on Respiratory Alkalosis and Insulin Sensitivity in Cinnamon Supplemented Pigs. *Animals* **2020**, *10*, 690. [[CrossRef](#)] [[PubMed](#)]
153. Miao, L.; St Clair, D.K. Regulation of superoxide dismutase genes: Implications in disease. *Free Radic. Biol. Med.* **2009**, *47*, 344–356. [[CrossRef](#)] [[PubMed](#)]
154. Miao, Q.; Si, X.; Xie, Y.; Chen, L.; Liu, Z.; Liu, L.; Tang, X.; Zhang, H. Effects of acute heat stress at different ambient temperature on hepatic redox status in broilers. *Poult. Sci.* **2020**, *99*, 4113–4122. [[CrossRef](#)] [[PubMed](#)]
155. Ghazi Harsini, S.; Habibiyani, M.; Moeini, M.M.; Abdolmohammadi, A.R. Effects of dietary selenium, vitamin E, and their combination on growth, serum metabolites, and antioxidant defense system in skeletal muscle of broilers under heat stress. *Biol. Trace Elem. Res.* **2012**, *148*, 322–330. [[CrossRef](#)]
156. Xue, B.; Song, J.; Liu, L.; Luo, J.; Tian, G.; Yang, Y. Effect of epigallocatechin gallate on growth performance and antioxidant capacity in heat-stressed broilers. *Arch. Anim. Nutr.* **2017**, *71*, 362–372. [[CrossRef](#)]
157. Zhang, Z.Y.; Jia, G.Q.; Zuo, J.J.; Zhang, Y.; Lei, J.; Ren, L.; Feng, D.Y. Effects of constant and cyclic heat stress on muscle metabolism and meat quality of broiler breast fillet and thigh meat. *Poult. Sci.* **2012**, *91*, 2931–2937. [[CrossRef](#)]
158. Zeng, T.; Li, J.J.; Wang, D.Q.; Li, G.Q.; Wang, G.L.; Lu, L.Z. Effects of heat stress on antioxidant defense system, inflammatory injury, and heat shock proteins of Muscovy and Pekin ducks: Evidence for differential thermal sensitivities. *Cell Stress Chaperones* **2014**, *19*, 895–901. [[CrossRef](#)]
159. Gourgou, E.; Aggeli, I.K.; Beis, I.; Gaitanaki, C. Hyperthermia-induced Hsp70 and MT20 transcriptional upregulation are mediated by p38-MAPK and JNKs in *Mytilus galloprovincialis* (Lamarck); a pro-survival response. *J. Exp. Biol.* **2010**, *213*, 347–357. [[CrossRef](#)]
160. Murai, H.; Hiragami, F.; Kawamura, K.; Motoda, H.; Koike, Y.; Inoue, S.; Kumagishi, K.; Ohtsuka, A.; Kano, Y. Differential response of heat-shock-induced p38 MAPK and JNK activity in PC12 mutant and PC12 parental cells for differentiation and apoptosis. *Acta Med. Okayama* **2010**, *64*, 55–62. [[CrossRef](#)]
161. Qi, Z.; Qi, S.; Gui, L.; Shen, L.; Feng, Z. Daphnetin protects oxidative stress-induced neuronal apoptosis via regulation of MAPK signaling and HSP70 expression. *Oncol. Lett.* **2016**, *12*, 1959–1964. [[CrossRef](#)]
162. English, J.G.; Shellhammer, J.P.; Malahe, M.; McCarter, P.C.; Elston, T.C.; Dohleman, H.G. MAPK feedback encodes a switch and timer for tunable stress adaptation in yeast. *Sci. Signal.* **2015**, *8*, ra5. [[CrossRef](#)] [[PubMed](#)]
163. Banton, M.C.; Tunnacliffe, A. MAPK phosphorylation is implicated in the adaptation to desiccation stress in nematodes. *J. Exp. Biol.* **2012**, *215*, 4288–4298. [[CrossRef](#)] [[PubMed](#)]
164. Gehart, H.; Kumpf, S.; Ittner, A.; Ricci, R. MAPK signalling in cellular metabolism: Stress or wellness? *EMBO Rep.* **2010**, *11*, 834–840. [[CrossRef](#)] [[PubMed](#)]
165. Pogozelski, A.R.; Geng, T.; Li, P.; Yin, X.; Lira, V.A.; Zhang, M.; Chi, J.T.; Yan, Z. p38 γ mitogen-activated protein kinase is a key regulator in skeletal muscle metabolic adaptation in mice. *PLoS ONE* **2009**, *4*, e7934. [[CrossRef](#)]
166. Wang, Z.; Brecher, P. Salicylate inhibition of extracellular signal-regulated kinases and inducible nitric oxide synthase. *Hypertension* **1999**, *34*, 1259–1264. [[CrossRef](#)]
167. Wang, W.; Hu, Y.; Yang, C.; Zhu, S.; Wang, X.; Zhang, Z.; Deng, H. Decreased NAD Activates STAT3 and Integrin Pathways to Drive Epithelial-Mesenchymal Transition. *Mol. Cell. Proteom.* **2018**, *17*, 2005–2017. [[CrossRef](#)]
168. Oeckler, R.A.; Arcuino, E.; Ahmad, M.; Olson, S.C.; Wolin, M.S. Cytosolic NADH redox and thiol oxidation regulate pulmonary arterial force through ERK MAP kinase. *Am. J. Physiol. Lung Cell. Mol. Physiol.* **2005**, *288*, L1017–L1025. [[CrossRef](#)]
169. Huwiler, A.; Wartmann, M.; van den Bosch, H.; Pfeilschifter, J. Extracellular nucleotides activate the p38-stress-activated protein kinase cascade in glomerular mesangial cells. *Br. J. Pharmacol.* **2000**, *129*, 612–618. [[CrossRef](#)]
170. Papa, S.; Choy, P.M.; Bubici, C. The ERK and JNK pathways in the regulation of metabolic reprogramming. *Oncogene* **2019**, *38*, 2223–2240. [[CrossRef](#)]